Coevolução em redes mutualistas: fluxo gênico e mosaicos de seleção

Coevolution in mutualistic networks: gene flow and selection mosaics

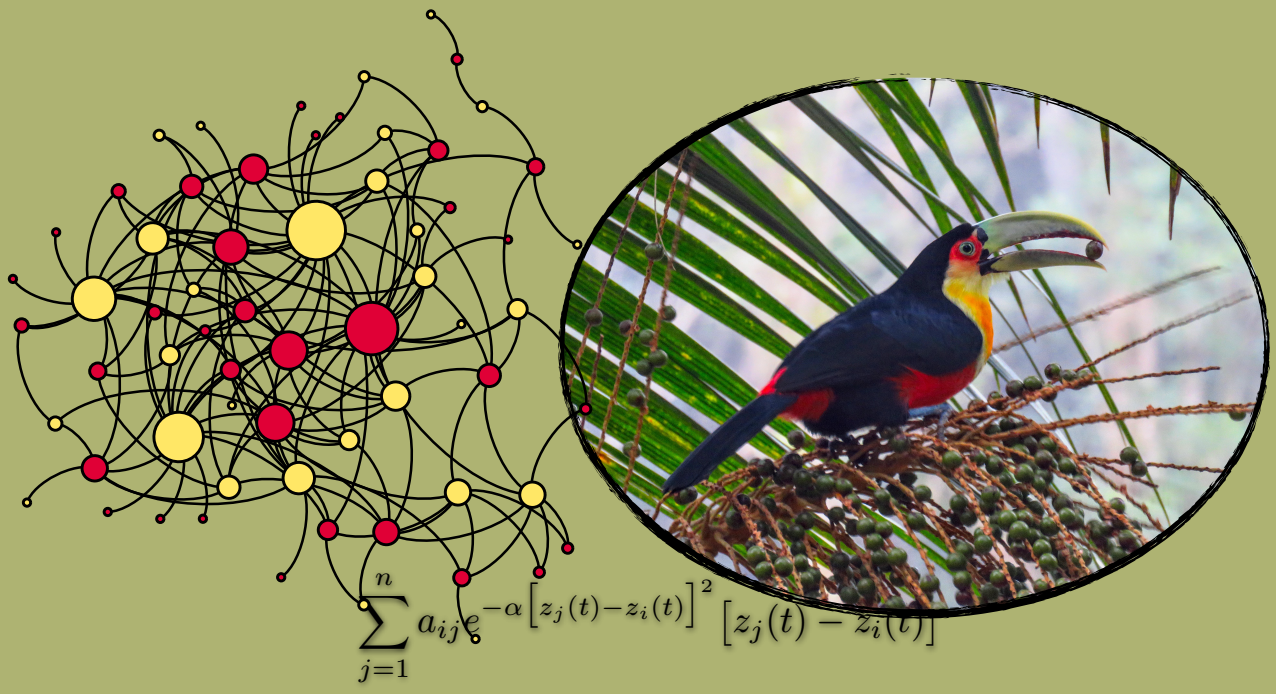

Lucas Paoliello de Medeiros

São Paulo
2017

Lucas Paoliello de Medeiros

Coevolução em redes mutualistas: fluxo gênico e mosaicos de seleção

Coevolution in mutualistic networks: gene flow and selection mosaics

Dissertação apresentada ao Instituto de Biociências da Universidade de São Paulo, para a obtenção de título de Mestre em Ciências na área de Ecologia.

Orientador: Prof. Dr. Paulo Roberto Guimarães Junior

São Paulo

2017

Ficha catalográfica

Medeiros, Lucas Paoliello de

Coevolução em redes mutualistas: fluxo gênico e mosaicos de seleção

65 páginas

Dissertação (Mestrado) — Instituto de Biociências da Universidade de São Paulo, Departamento de Ecologia.

1. Mosaico geográfico da coevolução; 2. Redes ecológicas; 3. Mutualismos

I. Universidade de São Paulo. Instituto de Biociências. Departamento de Ecologia.

Comissão Julgadora:

_____ _____

Prof(a). Dr(a). Prof(a). Dr(a).

_____

Prof(a). Dr(a).

_____

Prof. Dr. Paulo Roberto Guimarães Junior

(Orientador)

Ao meu avô Geraldo,

por me inspirar a ser cientista

"Hence, between the vast, macroscopic systems for which universal laws hold sway and the simple systems that can be analyzed using the fundamental laws of nature, there is a substantial middle ground of systems that are too complex for fundamental analysis but too simple to be universal — plenty of room, in short, for all the complexities of life as we know it."

Terence Tao

Agradecimentos

O trabalho que desenvolvi em meu mestrado e que resultou nesta dissertação não teria sido possível sem o apoio de diversas pessoas e instituições. Em primeiro lugar eu gostaria de agradecer imensamente ao Paulo "Miúdo" Guimarães. Miúdo, você foi o melhor orientador que eu poderia ter. Além de ser extremamente atencioso e motivador como orientador, você me ensinou sobre todas as dimensões da ciência como profissão. Sou extremamente grato à você!

Ao longo dos últimos 4 anos tive a sorte de poder conviver com diversos colegas brilhantes que são membros ou ex-membros do Guimarães Lab. Agradeço principalmente a: Cecilia Andreazzi, Ana Paula Assis, Juli Astegiano, Irina Barros, Roberta Bonaldo, Gustavo "Ari" Burin, Lucas Camacho III, Marilia Gaiarsa, Guilherme "Pato" Garcia, Paulinha Lemos, Flavia Marquitti, Lucas "Taio" Nascimento e Rafael Raimundo. Meu mestrado não seria nem uma pequena fração do que é se eu não tivesse aprendido, discutido, recebido críticas e dado risada com vocês! Aproveito para agradecer ao Mathias Pires, o exímio fotógrafo que clicou o tucano da capa desta dissertação.

Além dos meus colegas de laboratório, gostaria de agradecer à colegas do Instituto de Biociências da USP. Agradeço em especial aos membros da LAGE, ao Ramiro "Raica" Araujo, à Diana Garcia, ao Diog(r)o Melo, ao Danilo Mori, à Luísa "Sin" Novara e à Monique Simon. Trocar ideias com vocês sobre temas diferentes do meu mestrado tomando café ou cerveja foi uma experiência fundamental para mim.

Durante meu mestrado aprendi muito com professores do Departamento de Ecologia e de outros institutos do Brasil e do exterior. Agradeço muito ao Paulo Inácio Prado e ao Renato Vicente pelas discussões e sugestões das reuniões do comitê. Agradeço ao Alexandre Adalardo, Rodrigo Cogni, Mauro Galetti, Glauco Machado e Adriana Martini pelas disciplinas sensacionais que oferecem para pós-graduação. Agradeço ao John Thompson e Pedro Jordano pela enorme humildade com que discutiram ciência comigo mais de uma vez.

Eu também gostaria de agradecer às pessoas que fazem parte das instituições que me ampararam. Sou grato aos funcionários do Departamento de Ecologia da USP,

em especial à Vera Lima, por toda a ajuda durante meu mestrado. Também agradeço à FAPESP (2015/12956-7) e ao CNPq (131177/2015-0) pelo apoio financeiro.

Por fim, eu gostaria de agradecer imensamente à minha família e aos meus amigos. Agradeço principalmente aos meus pais, Marcelo e Paula, que são as pessoas mais extraordinárias do mundo e sempre me incentivaram muito nas minhas escolhas de carreira. Agradeço aos meus irmãos Diogo, Pedro e Rodrigo e aos meus amigos por estarem sempre perto alegrando a minha vida. Não tenho palavras para agradecer à Lola. Meu amor, você foi a melhor companheira e parceira possível durante o meu mestrado. Você me motiva muito no meu sonho de me tornar cientista, muito obrigado!

Índice

Resumo

Interações ecológicas como predação, competição e mutualismo são importantes forças que influenciam a evolução de espécies. Chamamos de coevolução a mudança evolutiva recíproca em espécies que interagem. A Teoria do Mosaico Geográfico da Coevolução (TMGC) fornece um arcabouço teórico para entender como conjuntos de populações coevoluem ao longo do espaço. Dois aspectos fundamentais da TMGC são o fluxo gênico entre populações e a presença de mosaicos de seleção, isto é, conjuntos de locais com regimes de seleção particulares. Diversos estudos exploraram como o acoplamento entre fenótipos de diferentes espécies evolui em pares ou pequenos grupos de espécies. Entretanto, interações ecológicas frequentemente formam grandes redes que conectam dezenas de espécies presentes em uma comunidade. Em redes de mutualismos, por exemplo, a organização das interações pode influenciar processos ecológicos e evolutivos. Um próximo passo para a compreensão do processo coevolutivo consiste em investigar como aspectos da TMGC influenciam a evolução de espécies em redes de interações. Nesta dissertação, tentamos preencher esta lacuna usando um modelo matemático de coevolução, ferramentas de redes complexas e informação sobre redes mutualistas empíricas. Nossas simulações numéricas do modelo coevolutivo apontam para três principais conclusões. Primeiro, o fluxo gênico influencia os padrões fenotípicos gerados por coevolução e pode favorecer a emergência de acoplamento fenotípico entre espécies dependendo do mosaico de seleção. Segundo, a organização de redes mutualistas influencia a coevolução, mas este efeito pode desaparecer quando o fluxo gênico favorece acoplamento fenotípico. Mutualismos íntimos, como proteção de plantas hospedeiras por formigas, formam redes pequenas e compartimentalizadas que geram um maior acoplamento fenotípico do que as redes grandes e aninhadas típicas de mutualismos entre espécies de vida livre, como polinização. Por fim, a fragmentação de habitat, ao extinguir o fluxo gênico, pode reduzir as adaptações recíprocas entre espécies e ao mesmo tempo tornar cada espécie mais adaptada ao seu ambiente abiótico local. Em suma, mostramos que interações complexas entre fluxo gênico, estrutura geográfica da seleção e organização de redes ecológicas moldam a evolução de grandes grupos de espécies. Dessa forma, podemos traçar previsões sobre como impactos ambientais como a fragmentação de habitat irão alterar a evolução de interações ecológicas.

Abstract

Ecological interactions such as predation, competition, and mutualism are important forces that influence species evolution. Coevolution is defined as reciprocal evolutionary change in interacting species. The Geographic Mosaic Theory of Coevolution (GMTC) provides a theoretical framework to explain how collections of populations should coevolve across space. Two fundamental aspects of the GMTC are gene flow among populations and the presence of selection mosaics, which are collections of localities with particular selection regimes. Several studies have explored how phenotypic trait matching between species evolves in pairs or small groups of species. However, ecological interactions frequently form large networks that connect dozens of species present in a given community. In networks of mutualisms, for instance, the organization of interactions may affect ecological and evolutionary processes. A next step in understanding the coevolutionary process is to investigate how aspects of the GMTC affect the evolution of species embedded in interaction networks. In this dissertation, we tried to fill this gap using a mathematical model of coevolution, complex networks tools, and information on empirical mutualistic networks. Our numerical simulations of the coevolutionary model allow us to draw three main conclusions. First, gene flow affects trait patterns generated by coevolution and may favor the emergence of trait matching depending on the selection mosaic. Second, the organization of mutualistic networks influences coevolution, but this effect may vanish when gene flow favors trait matching. Intimate mutualisms, such as protection of host plants by ants, form small and compartmentalized networks that generate higher trait matching than large and nested networks typical of mutualisms among free-living species, such as pollination. Third, habitat fragmentation resulting in the disruption of gene flow should reduce the reciprocal adaptations between interacting species and at the same time promote adaptations to the local abiotic environment. In conclusion, we show that a complex interplay between gene flow, the geographic structure of selection, and the organization of ecological networks shapes the evolution of large groups of species. Our results therefore allow predictions of how environmental impacts such as habitat fragmentation will modify the evolution of species interactions.

Gene flow and selection mosaics shape coevolution in mutualistic networks

Lucas P. Medeiros & Paulo R. Guimarães Jr.

Departamento de Ecologia, Instituto de Biociências, Universidade de São Paulo, Rua do Matão, Travessa 14, no. 321, CEP: 05508-900, São Paulo, SP, Brazil

Keywords: Ecological networks, geographic mosaic, interaction intimacy, mutualism, trait matching, species interactions

Statement of authorship: LPM and PRG conceived and designed the study. LPM and PRG developed the mathematical model. LPM conducted the numerical simulations and analyses. LPM wrote the manuscript with substantial input from PRG.

Abstract

Coevolution is considered a major force shaping the traits of interacting species. Processes of the geographic mosaic of coevolution such as gene flow and selection mosaics have been shown to be of central importance for coevolution. Furthermore, work on multispecies coevolution show that additional interacting species may dramatically alter pairwise coevolution. However, the specific roles of the geographic mosaic of coevolution in species-rich systems are largely unexplored. Here, we fill this gap for mutualisms by combining a mathematical model of coevolution, network tools, and information on empirical mutualistic networks to investigate how gene flow and selection mosaics affect trait patterns generated by coevolution. Our simulation results allow us to draw three main conclusions. First, gene flow affects trait patterns generated by coevolution and may favor the emergence of trait matching depending on the selection mosaic. Second, the network structure of different mutualisms affects coevolution in distinct ways, but the effect of network structure may vanish when gene flow favors trait matching. Third, habitat fragmentation resulting in the disruption of gene flow should reduce the coadaptations between mutualistic partners and promote adaptations to the local abiotic environment. This set of results provides clear predictions of how the geographic mosaic shapes species-rich interactions often considered diffuse and how the widespread fragmentation of natural landscapes may modify the coevolutionary process.

Introduction

Ecological interactions among species constitute one of major forces organizing the Earth's biodiversity (Thompson 2005). Interacting species may influence each other's population dynamics (Krebs *et al.* 1995; Frederickson & Gordon 2009), phenotypic trait evolution (Grant & Grant 2006; Gervasi & Schiestl 2017), and diversification dynamics (Ramírez *et al.* 2011; Silvestro *et al.* 2015). When two interacting species exert selection upon each other such reciprocal selection may lead to coevolution, the reciprocal evolutionary change between interacting species. An extensive amount of research has shown that coevolution is capable of producing adaptation and coadaptation in interacting pairs of species via a variety of dynamics (Thompson 2005). In the last few decades, coevolutionary research has broaden its scope to embrace the notion that the majority of interacting pairs of species co-occur at several distinct localities and are often embedded in even larger interacting assemblages (Iwao & Rausher 1997; Thompson & Cunningham 2002; Strauss & Irwin 2004; Benkman *et al.* 2013; Newman *et al.* 2014). Unraveling this geographical and ecological complexity of the coevolutionary process constitutes a major challenge at the interface of ecology and evolution (Thompson 2009).

Spatial processes such as gene flow and metapopulation dynamics connect populations from the same species that are subject to distinct local evolutionary forces and may alter evolutionary dynamics in profound ways (Gandon 2002; Lenormand 2002). Gene flow, for instance, may either preclude phenotypic differentiation between different populations or promote adaptive evolution by increasing local genetic variation (Hendry & Taylor 2004; Fitzpatrick *et al.* 2015). The processes and patterns involved in the coevolution of connected populations across landscapes has been organized by the Geographic Mosaic Theory of Coevolution (GMTC; Thompson 2005). Central to the GMTC is the concept of a selection mosaic, which is a collection of localities exhibiting particular selection regimes for interacting species. In particular, two kinds of regimes constitute the core of selection mosaics: (i) hotspots, in which selection is reciprocal between interacting species and (ii) coldspots, in which at least one of the species is not under selection imposed by the other species. Selection mosaics are usually associated with variation in community context as has been estimated for a wide range of interactions including pollinating seed parasites and plants (Thompson & Cunningham 2002), seed-eating birds and

conifers (Benkman *et al.* 2003), protective ants and plants with extrafloral nectaries (Rudgers & Strauss 2004), and plants with both herbivores and pollinators (Gómez *et al.* 2009).

The combination of selection mosaics, hotspots and coldspots, and processes that remix species traits across space such as gene flow may lead to differentiation among populations in the traits mediating the interaction and to trait mismatching in some localities (Thompson 2005). We now know that geographical variation in traits and trait mismatching in pairwise interactions emerge as a result of one or more processes of the GMTC (Anderson & Johnson 2008; Hanifin *et al.* 2008). A next step to further understand the coevolutionary process is to investigate how trait matching and mismatching are distributed across a landscape for species-rich assemblages. In this sense, quantitative tools that deal with multiple selection pressures acting on species embedded in large ecological assemblages are needed to improve our understanding of coevolution in a spatial context.

Network theory provides tools to investigate the organization of interactions and the ecological and evolutionary dynamics of species-rich assemblages (Jordano 1987; Thompson 2005; Ings *et al.* 2009). Particular interest has been devoted to mutualisms, which frequently form small to large networks that connect the species present at a given community (Bascompte & Jordano 2014). Such mutualistic networks greatly vary in the organization of interactions depending on the degree of physiological integration as well as physical and trophic dependence between interacting partners (i.e. the interaction intimacy; Ollerton 2006; Guimarães *et al.* 2007a; Fontaine *et al.* 2011). Mutualisms with low interaction intimacy (hereafter low-intimacy mutualisms) such as seed dispersal by fruiting-eating vertebrates generate large networks with high heterogeneity in the number of partners of different species (Jordano 1987; Bascompte *et al.* 2003; Guimarães *et al.* 2007b). On the other hand, mutualisms with high interaction intimacy (hereafter high-intimacy mutualisms) such as the protection of host plants (myrmecophytes) by defensive ants are characterized by small networks with semi-isolated groups of interacting species (Fonseca & Ganade 1996; Ricciardi *et al.* 2010; Dáttilo *et al.* 2013b). Such differences in network architecture indicate that different ecological and evolutionary processes shape patterns of interaction at the community level in different mutualisms (Blüthgen *et al.* 2007; Guimarães *et al.* 2007a; Raimundo *et al.* 2014).

The evolution of species traits in mutualistic networks has only been explicitly investigated in a handful of theoretical studies (Santamaría & Rodríguez-Gironés 2007; Loeuille 2010; Guimarães *et al.* 2011; Nuismer *et al.* 2013). When coevolutionary selection is based on trait complementarity such as the match between a plant's corolla and a pollinating hummingbird's bill trait complementarity and trait convergence (i.e. trait similarity in unrelated species) increase in mutualistic networks (Guimarães *et al.* 2011). Furthermore, super-generalist species that interact with a disproportionate number of other species modify the network structure and fuel the emergence of trait complementarity and trait convergence (Guimarães *et al.* 2011). Nevertheless, the emergence of these trait patterns may depend on the strength and type of mutualistic selection (Nuismer *et al.* 2013). Because Guimarães *et al.* (2011) and Nuismer *et al.* (2013) only explored pollination and seed-dispersal networks, one question that remains unanswered is whether networks formed by high-intimacy mutualisms would promote similar coevolutionary dynamics. It is unclear, for example, whether the reciprocal specialization between species within semi-isolated groups in high-intimacy mutualisms should favor higher levels of trait matching than the centralization promoted by generalist species in low-intimacy mutualisms.

Given that ecological networks often show spatial variation in species composition and structural aspects (Dáttilo *et al.* 2013a; Carstensen *et al.* 2014; Gilarranz *et al.* 2015; Trojelsgaard *et al.* 2015), it is expected that selection should greatly vary at different localities. It is also expected that spatial processes will be even more crucial for the ecology and evolution of multispecies systems with the widespread habitat fragmentation driven by human action (Hagen *et al.* 2012; Cheptou *et al.* 2017). Across a given landscape with several mutualistic networks, coevolution should generate higher levels of trait matching at localities where mutualism is an important selection pressure (i.e. hotspots) than at localities where other biotic or abiotic factors exert greater selection (i.e. coldspots; Fig. 1a). Additionally, it is reasonable to expect that gene flow should homogenize species traits across the landscape (Fig. 1b). However, understanding how the interplay between gene flow, selection mosaics, and multiple selection pressures shapes trait matching patterns at different localities is a current major challenge for coevolutionary research.

In this study, we bridge the conceptual framework of the GMTC with ecological network theory to understand how species coevolve in multispecies ecological assemblages across landscapes. We combined a mathematical model of single-trait evolution, network tools, and a comprehensive dataset of empirical networks to investigate the effects of gene flow and selection mosaics on network- and species-level trait patterns generated by coevolution. We concentrated on three central questions: (i) How does gene flow and geographical variation in the selection imposed by mutualism affect the trait matching between interacting species generated by coevolution? (ii) How does the network structure of different kinds of mutualisms mediate the coevolutionary effects of gene flow and geographical variation in the selection imposed by mutualism? (iii) What are the coevolutionary consequences of habitat fragmentation that results in the disruption of gene flow to the adaptation of species to their mutualistic partners and to their local environment?

Material and methods

Dataset

Our dataset consisted of 72 empirical mutualistic networks, which represent the recorded interactions between species at a given locality through extensive fieldwork (Table S1). Our dataset had a broad geographic and taxonomic span and included eight types of mutualisms. These types of mutualisms can be divided in two broad categories according to their degree of interaction intimacy (Ollerton 2006; Guimarães *et al.* 2007a; Fontaine *et al.* 2011; Raimundo *et al.* 2014). First, high-intimacy mutualisms: (i) anemones that protect anemonefishes (n = 11 networks) and (ii) ants that protect their host plants, the myrmecophytes (n = 8). Second, low-intimacy mutualisms: (iii) ants that protect plants with extrafloral nectaries (EFN; n = 5), (iv) insects and vertebrates that pollinate flowering plants (n = 28), (v) fruit-eating vertebrates that disperse the seeds of plants with fleshy fruits (n = 17), and (vi) fishes and shrimps that clean client fishes (n = 3). The majority of networks is published and available online as described in Table S1. Some of the networks are from unpublished datasets and were used by us with the kind permission of Victor Rico-Gray, Cristina Sazima, Ivan Sazima, and Thiago Izzo (Table S1).

Network structure

We quantified five widely used metrics of network structure to characterize the arrangement of interactions in our networks: (i) species richness (R), (ii) degree variance (σ_k^2), (iii) connectance (C), (iv) nestedness ($NODF$), and (v) modularity (Q; Supporting Information). For these analyses we represented each network as a bipartite adjacency matrix that defines the interactions between two distinct sets of species (e.g. pollinators and plants; Supporting Information). Although some of our networks have information on interaction strength, we decided to use only the information on presence and absence of interactions (i.e. 1 and 0) in order to use the same type of data for all our networks and because the interaction strengths evolve in our coevolution model (see below). Degree variance is defined as the variance of all degree values (i.e. the number of interaction partners of a species) and measures the heterogeneity in the number of partners in the network. Connectance is the proportion of all possible interactions that are in fact realized and represents how well connected species are to each other in the network (Jordano 1987). Nestedness measures how much the interactions of species with low degree values are proper subsets of the interactions of species from the same set that have higher degree values (Bascompte *et al.* 2003). We quantified nestedness using the metric *NODF*, which varies from 0 (no nestedness) to 1 (perfect nestedness; Almeida-Neto *et al.* 2008). Finally, modularity measures how much the network is partitioned in groups of species (i.e. modules) with many interactions within groups and few interactions among different groups (Olesen *et al.* 2007). We computed modularity using a simulated annealing algorithm to optimize the value of a bipartite version of the metric Q, which varies from 0 (no modularity) to 1 (perfect modularity; Barber 2007; Marquitti *et al.* 2013). Nestedness and modularity are known to be affected by other network properties (Bascompte *et al.* 2003; Fortuna *et al.* 2010). To control the effects of network richness, degree variance, and connectance on nestedness and modularity, we standardized the *NODF* and Q values using null models (Supporting Information).

Because network structural metrics are often highly correlated among each other (Jordano 1987; Bascompte *et al.* 2003; Fortuna *et al.* 2010), we used principal component analysis (PCA) to describe how the values of our five metrics covary across networks. We used the correlation matrix among our five metrics in the PCA because of large differences in the scale of our metrics (Table S1). By using PCA, we

were able to obtain two axes of structural variation — the first two principal components (*PC1* and *PC2*) — that describe the variation in network structure of our dataset. We used our values of *PC1* and *PC2* to explore how network structure affects the outcome of coevolution. Modularity was calculated using the program MODULAR (Marquitti *et al.* 2014) and the other metrics were calculated in R 3.3.2 (Dormann *et al.* 2008; R Core Team 2016).

Coevolution model for one locality

We developed a mathematical model of coevolution based on previous theory on evolution in ecological networks (Guimarães *et al.* 2011; Nuismer *et al.* 2013; Andreazzi *et al.* 2017) In our model, we represented each of the R_A species that engage in a given mutualism at locality *A* as a single population. We modeled the evolution by natural selection of the mean value ($\bar{z}_{i,A}$) of a single trait z_i of each species *i* (Fig. 1). We assumed that population sizes are large enough for genetic drift to be negligible. We also assumed that the phenotypic variance of trait z_i, $\sigma^2_{z_i,A}$, is fixed through time, which is a reasonable approximation if population sizes are large and selection does not erode genetic variance. We considered that trait z_i mediates mutualistic interactions between individuals (e.g. hummingbird bill length, flower corolla length) and affects the fitness benefits of mutualism. In addition to mutualism, z_i also determines fitness components related to abiotic factors and other ecological interactions (Nuismer *et al.* 2010, 2013; Andreazzi *et al.* 2017). Thus, z_i is under selection imposed by mutualism (hereafter mutualistic selection) and selection imposed by abiotic factors and other ecological interactions (hereafter environmental selection; Fig. 1).

In our model, the change in the mean trait value of species *i* at locality *A* between generation $t + 1$ and generation *t* was derived using the classical equation by Lande (1976): $\Delta\bar{z}_{i,A}(t) = h^2_{z_i,A}\sigma^2_{z_i,A}\frac{\partial \ln \bar{W}_{i,A}}{\partial \bar{z}_{i,A}(t)}$. Here, $h^2_{z_i,A}$ ($0 \leq h^2_{z_i,A} \leq 1$) is the trait heritability that we assumed to be constant over time and $\frac{\partial \ln \bar{W}_{i,A}}{\partial \bar{z}_{i,A}(t)}$ is the selection gradient. To describe an adaptive landscape related to mutualistic and environmental selection we defined a linear selection gradient as follows: $\frac{\partial \ln \bar{W}_{i,A}}{\partial \bar{z}_{i,A}(t)} = \rho_{i,A}\left[z'_{i,A}(t) - \bar{z}_{i,A}(t)\right]$, where $\rho_{i,A}$ is a scaling constant that relates changes in mean fitness to

changes in mean trait values and $z'_{i,A}(t)$ is the trait value that defines the adaptive peak of the population at generation *t*. We decomposed $z'_{i,A}(t)$ into two components, one related to mutualism and one related to the environment: $z'_{i,A}(t) = m_{i,A}\sum_{j,j\neq i}^{R_A} q_{ij,A}(t)x_{ij,A}(t) + \left(1 - m_{i,A}\right)\theta_{i,A}(t)$. Here, $m_{i,A}$ measures the relative importance of mutualism as a selection pressure ($0 \leq m_{i,A} \leq 1$), $q_{ij,A}(t)$ represents the evolutionary importance of species *j* to species *i*, $x_{ij,A}(t)$ is the mean trait value of species *i* favored by selection imposed by species *j*, and $\theta_{i,A}(t)$ is the mean trait value favored by environmental selection (Fig. 1).

We used two additional assumptions to obtain a final equation describing the dynamics of trait z_i at a single locality. First, we supposed that the trait value selected by the environment is fixed over time ($\theta_{i,A}(t) = \theta_{i,A}$). Second, we assumed that mutualistic selection favors the complementarity of traits (i.e. phenotype matching, Nuismer *et al.* 2010, 2013). Thus, the selected trait value with respect to partner *j* at generation *t* is $\bar{z}_{j,A}(t) = x_{ij,A}(t)$, which corresponds to the value that maximizes the trait matching between $z_{i,A}$ and $z_{j,A}$. Using our equations for the adaptive landscape and the fact that $h^2_{z_i,A} = \sigma^2_{G_{z_i,A}}/\sigma^2_{z_i,A}$, in which $\sigma^2_{G_{z_i,A}}$ is the additive genetic variance of trait z_i, the dynamics of trait z_i may be described as follows:

$$\Delta\bar{z}_{i,A}(t) = \varphi_{i,A}\left\{m_{i,A}\sum_{j,j\neq i}^{R_A} q_{ij,A}(t)\left[\bar{z}_{j,A}(t) - \bar{z}_{i,A}(t)\right] + \left(1 - m_{i,A}\right)\left[\theta_{i,A} - \bar{z}_{i,A}(t)\right]\right\} \qquad (1),$$

in which $\varphi_{i,A}$ is a compound parameter ($\varphi_{i,A} = \sigma^2_{G_{z_i,A}}\rho_{i,A}$).

We now describe how $q_{ij,A}(t)$ changes through time. The term $q_{ij,A}(t)$ represents the evolutionary importance of species *j* to species *i* in relation to all other mutualistic partners of *i* ($0 \leq q_{ij,A}(t) \leq 1$ and $\sum_{j,j\neq i}^{R_A} q_{ij,A}(t) = 1$). The term $q_{ij,A}(t)$ has two components that represent how different traits mediate the fitness consequences of the mutualism. First, the component $e^{-\alpha\left(\bar{z}_{j,A}(t) - \bar{z}_{i,A}(t)\right)^2}$ is associated with trait z_i and represents the magnitude of trait matching between species *i* and *j*. This component is 1 when there is maximum matching ($\bar{z}_{i,A} = \bar{z}_{j,A}$) and approximates 0 if there is poor matching. The parameter α represents the sensitivity of mutualistic selection to trait matching and was assumed to be the same for every species and to be fixed over time. Second, the component $a_{ij}(t)$ encapsulates the effects of a suite of other traits not

explicitly modeled by us and defines if an interaction is allowed to occur (i.e. $a_{ij}(t) = 1$) or represents a forbidden link (i.e. $a_{ij}(t) = 0$) between i and j. We assumed that z_i evolves a faster rate than all other traits related to the mutualism and, therefore, $a_{ij}(t)$ may be considered fixed in our model ($a_{ij}(t) = a_{ij}$). In our simulations, we parameterized a_{ij} using our empirical mutualistic networks. Therefore, a_{ij} imposes a fixed structure of potential interactions, while $e^{-\alpha\left(\bar{z}_{j,A}(t)-\bar{z}_{i,A}(t)\right)^2}$ defines a dynamic structure of the evolutionary strength of interactions. Thus, $q_{ij,A}(t)$ is given by:

$$q_{ij,A}(t) = \frac{a_{ij}e^{-\alpha\left(\bar{z}_{j,A}(t)-\bar{z}_{i,A}(t)\right)^2}}{\sum_{k,k\neq i}^{R_A} a_{ik}e^{-\alpha\left(\bar{z}_{k,A}(t)-\bar{z}_{i,A}(t)\right)^2}} \quad (2).$$

Coevolution model for two localities

We now extend our model to a scenario in which there are two localities and there may be gene flow between the populations of the same species that occur at both localities (Fig. 1b). We considered that, at generation t, a fraction $g_i(t)$ of the population of species i migrates from locality A to locality B and from locality B to locality A and a fraction ($1 - g_i(t)$) remains at its own locality. Therefore, we supposed that migration is symmetric between localities, which would not alter the population sizes through time. We also assumed that local individuals and migrants mate randomly, which allowed us to use $g_i(t)$ as a measure of gene flow. Although $g_i(t)$ may depend on species traits and therefore vary over time, we assumed that migration ability is a fixed property of each species, which allowed us to use $g_i(t) = g_i$. Using a final assumption that φ_i is the same for both populations of the same species, we defined a new equation for the evolutionary change in $\bar{z}_{i,A}$:

$$\begin{aligned}\Delta\bar{z}_{i,A}(t) = (1-g_i)\varphi_i\left\{m_{i,A}\sum_{j,j\neq i}^{R_A} q_{ij,A}(t)\left[\bar{z}_{j,A}(t)-\bar{z}_{i,A}(t)\right] + \left(1-m_{i,A}\right)\left[\theta_{i,A}-\bar{z}_{i,A}(t)\right]\right\} \\ + g_i\varphi_i\left\{m_{i,B}\sum_{j,j\neq i}^{R_B} q_{ij,B}(t)\left[\bar{z}_{j,B}(t)-\bar{z}_{i,B}(t)\right] + \left(1-m_{i,B}\right)\left[\theta_{i,B}-\bar{z}_{i,B}(t)\right]\right\}\end{aligned} \quad (3).$$

The equation for $\bar{z}_{i,B}$ is obtained by exchanging the subscript A for B and vice versa in equation (3). In our simulations, we used equation (3) to explore the effects of gene flow (g_i) and geographical variation in mutualistic selection ($m_{i,A}$ and $m_{i,B}$) on coevolution.

Our model is general enough to allow for differences in species composition and network structure between localities *A* and *B*. However, we restrict our analyses to the case in which both localities have the same species composition (i.e. $R_A = R_B$) and the same adjacency matrix describing mutualistic interactions. Although a_{ij} is the same at both localities, the parameters m_i and θ_i may vary between the two populations of each species *i*, generating distinct adaptive landscapes for each population.

Characterization of trait patterns

We used three metrics to describe network- and species-level trait patterns that could be affected by coevolution. The first metric measures the degree of adaptation of each species to its mutualistic partners and was termed trait matching. Trait matching was calculated for each pair of interacting species *i* and *j* at locality *A* in generation t as $\tau_{ij,A}(t) = e^{-\alpha\left(\bar{z}_{j,A}(t)-\bar{z}_{i,A}(t)\right)^2}$. Because this metric is based on the difference between the traits of *i* and *j*, it is highly correlated with the metric of trait complementarity used by Guimarães *et al.* (2011; results not shown). The second metric quantifies the degree of adaptation of each species to its local environment and was called environmental matching. Environmental matching was calculated for species *i* at locality *A* in generation t as $\varepsilon_{i,A}(t) = e^{-\alpha\left(\theta_{i,A}-\bar{z}_{i,A}(t)\right)^2}$. Trait matching and environmental matching at locality *B* have an equivalent definition. Finally, the third metric measures the degree of trait divergence between two populations of the same species and was termed geographical divergence. Geographical divergence was calculated for species *i* in generation *t* as $\delta_i(t) = e^{-\alpha\left(\bar{z}_{i,B}(t)-\bar{z}_{i,A}(t)\right)^2}$. Using the pairwise values for $\tau_{ij,A}(t)$ and the values of $\varepsilon_{i,A}(t)$ and $\delta_i(t)$ for each species, we also calculated the network-level mean values ($\bar{\tau}_A(t)$, $\bar{\varepsilon}_A(t)$, and $\bar{\delta}(t)$) and the standard deviation ($\sigma_{\tau_A}(t)$, $\sigma_{\varepsilon_A}(t)$, and $\sigma_\delta(t)$) of these metrics in each generation *t*.

Numerical simulations and statistical analyses

We performed numerical simulations of our coevolution model to investigate how gene flow (g_i), geographic variation in mutualistic selection ($m_{i,A}$ and $m_{i,B}$), and network structure (*PC1* and *PC2*) affect the emergence of trait patterns. We performed

three sets of simulations that are described in the following paragraphs. In the beginning of all simulations, we sampled parameter values for each species *i* according to the following distributions: (i) g_i: truncated normal distribution between 0 and 1 with mean = $\bar{g}$ and sd = 0.001, (ii) $m_{i,A}$ ($m_{i,B}$): truncated normal distribution between 0 and 1 with mean = $\overline{m}_A$ ($\overline{m}_B$) and sd = 0.01, (iii) φ_i: truncated normal distribution between 0 and 1 with mean = 0.2 and sd = 0.01, and (iv) $\theta_{i,A}$ ($\theta_{i,B}$): uniform distribution with range [0, 20] ([20, 40] for locality *B*). We set $g_i = \bar{g}$, $m_{i,A} = \overline{m}_A$, or $m_{i,B} = \overline{m}_B$ for every species *i* whenever the mean value ($\bar{g}$, $\overline{m}_A$, or $\overline{m}_B$) was either 0 or 1 to avoid sampling problems. In addition, we used $\alpha = 0.2$ for all simulations. We decided to use a fixed value for α and for the mean value of φ_i in all our simulations because previous work shows that analogous parameters have a weak effect on coevolutionary dynamics (Guimarães *et al.* 2011; Andreazzi *et al.* 2017). Our distributions for $\theta_{i,A}$ and $\theta_{i,B}$ were chosen to explore a scenario in which different communities present contrasting environments as is observed for many kinds of interacting species (Thompson 2005; Anderson & Johnson 2008; Piculell *et al.* 2008; Gómez *et al.* 2009). In all simulations, species started at the selected trait value in relation to the environment ($\bar{z}_{i,A}(0) = \theta_{i,A}$ and $\bar{z}_{i,B}(0) = \theta_{i,B}$). Simulations ran until the average difference $\left|\bar{z}_{i,A}(t) - \bar{z}_{i,A}(t+1)\right|$ for all species *i* at both localities was less than 10^{-6} or until 10^4 generations were reached. This condition was sufficient to reach equilibrium in trait values (Fig. S1, S2). We recorded the values of trait matching (τ_{ij}), environmental matching (ε_i), and geographical divergence (δ_i) at both localities in the beginning and end of each simulation.

We now describe our three sets of simulations. In our first set of simulations we explored five scenarios of selection mosaics: (i) $\overline{m}_A = \overline{m}_B = 0.9$; (ii) $\overline{m}_A = 0.9$ and $\overline{m}_B = 0.7$; (iii) $\overline{m}_A = 0.9$ and $\overline{m}_B = 0.5$; (iv) $\overline{m}_A = 0.9$ and $\overline{m}_B = 0.3$; (v) $\overline{m}_A = 0.9$ and $\overline{m}_B = 0.1$. We focused our analyses on scenario (i), which represents two hotspots, and scenario (v), which represents one hotspot (locality *A*) and one coldspot (locality *B*). For each scenario, we used 21 different values of mean gene flow ($\bar{g}$) between 0 and 0.1 in increments of 0.005. We performed 100 simulations for each of our 72 empirical networks per combination of selection mosaic and gene flow (n = 756,000 simulations). We performed statistical tests to investigate the effects of mutualism type, degree of interaction intimacy, mean value of gene flow ($\bar{g}$), and network structure (*PC1* and *PC2*) on the network-level trait matching ($\bar{\tau}$) at the end of

simulations. We are aware of the issues regarding statistical testing using simulation data (White *et al.* 2014). Here, we performed statistical tests to have a measure of the effect size of each parameter or factor of interest to us and we do not ground our conclusions on significance (i.e. p-values). We used one-way ANOVA to test for differences among different mutualisms in the mean value for 100 simulations per network of the network-level trait matching ($\bar{\tau}_{n=100}$). We used t-tests to test if $\bar{\tau}_{n=100}$ differed between high-intimacy and low-intimacy mutualisms. We used linear mixed models to test for the effects of gene flow and mutualism type on $\bar{\tau}_{n=100}$. In our models, $\bar{\tau}_{n=100}$ was our response variable and gene flow, mutualism type, and the interaction between gene flow and mutualism type were our three predictor variables. In this analysis we used only two values of $\bar{g}$ (0 and 0.1) in order to obtain a simple effect size of gene flow on coevolution. We defined the network identity as a random effect in our linear mixed model. Finally, we used linear regression to test for the effects of network structure (either *PC1* or *PC2*) on $\bar{\tau}_{n=100}$. We fitted separate regressions for three different values of gene flow ($\bar{g}$ = 0, $\bar{g}$ = 0.01, $\bar{g}$ = 0.1). Because our previous statistical analyses showed that high- and low-intimacy mutualisms generate disparate degrees of trait matching, we also fitted separate regressions for high- and low-intimacy mutualisms.

In our second set of simulations we explored a larger region of the parameter space for two networks with contrasting structures (networks 29 and 65 in Table S1). To do so we defined 882 combinations of $\overline{m}_A$, $\overline{m}_B$, and $\bar{g}$. Combinations of $\overline{m}_A$ and $\overline{m}_B$ were either symmetric ($\overline{m}_A = \overline{m}_B$ for $\overline{m}_A$ between 0 and 1 in increments of 0.05) or asymmetric ($\overline{m}_A = 1 - \overline{m}_B$ for $\overline{m}_A$ between 0 and 1 in increments of 0.05). For each combination of $\overline{m}_A$ and $\overline{m}_B$, we explored 21 different values of mean gene flow ($\bar{g}$) between 0 and 0.1 in increments of 0.005. We performed 100 simulations per network for each combination of $\overline{m}_A$, $\overline{m}_B$, and $\bar{g}$ (n = 176,400 simulations).

Finally, our third set of simulations aimed to verify the coevolutionary effects of habitat fragmentation by removing the gene flow between two connected hotspots ($\overline{m}_A = \overline{m}_B = 0.9$). In these simulations traits evolved to equilibrium with high gene flow ($\bar{g}$ = 0.1) and then gene flow was removed ($\bar{g}$ = 0) and coevolution proceeded to a new equilibrium. We performed 100 simulations for each of our 72 empirical networks (n = 7,200 simulations). We used linear mixed models to test for the effects of gene flow and mutualism type on the emergence of trait matching ($\bar{\tau}_{n=100}$) and environmental

matching ($\bar{\varepsilon}_{n=100}$). The structure of these models was identical to the linear mixed models used for our first set of simulations (see above). All simulations and statistical analyses were done in R 3.3.2 (Bates *et al.* 2015; R Core Team 2016).

Results

Effects of gene flow and selection mosaics on coevolution

Coevolution in our numerical simulations always proceeded to an equilibrium in which trait values remain fixed over time (Fig. S1, S2). When the selection mosaic consisted of two isolated hotspots ($\overline{m}_A = \overline{m}_B = 0.9, \bar{g} = 0$), the network-level trait matching ($\bar{\tau}$) at equilibrium at a given locality was higher for high-intimacy than for low-intimacy mutualisms (high-intimacy: $\bar{\tau}_{A,n=100} = 0.85 \pm 0.05$ vs. low-intimacy: $\bar{\tau}_{A,n=100} = 0.66 \pm 0.09$, mean $\pm$ sd; Welch two sample t-test: $t_{56.95} = 11.09$, $p < 0.0001$; $\bar{\tau}_{A,n=100}$: mean value for 100 simulations per network of the network-level trait matching at locality *A*; Fig. 2a). In addition, trait matching greatly differed between different mutualisms in isolated hotspots (ANOVA: $F_{5, 66} = 17.43$, $p < 0.0001$; Fig. 2a). In particular, ant-myrmecophyte networks generated the highest levels of trait matching ($\bar{\tau}_{A,n=100} = 0.88 \pm 0.06, \bar{g} = 0$) and frugivore-plant networks generated the lowest levels of trait matching ($\bar{\tau}_{A,n=100} = 0.62 \pm 0.09, \bar{g} = 0$).

Gene flow between two hotspots affected how coevolution leads to trait matching in two main ways. First, gene flow had an unexpected effect of increasing trait matching (Likelihood ratio test for linear mixed model: $\chi^2(1) = 111.64$, $p < 0.0001$; Table S2). Furthermore, trait matching was higher for high-intimacy mutualisms ($\chi^2(5) = 59.92$, $p < 0.0001$), but the effect of gene flow was stronger for low-intimacy mutualisms ($\chi^2(5) = 58.24$, $p < 0.0001$; Fig 2a; Table S2). Second, gene flow decreased the variation in the network-level trait matching across different networks, especially for low-intimacy mutualisms (Fig. 2a). The change in the network-level trait matching ($\bar{\tau}$) in a given simulation is the outcome of changes in the trait matching of pairwise interactions (τ_{ij}). We observed that gene flow increases the network-level trait matching in two hotspots by increasing the trait matching of poorly matched pairs of species, spreading coadaptation throughout the network (Fig. S3). Thus, gene flow increases mean pairwise matching and reduces the standard

deviation in pairwise matching (σ_τ) and this effect is stronger for low-intimacy mutualisms (Fig. S4).

We also explored the coevolutionary dynamics when a network in which mutualism is a strong selective pressure (hotspot: $\overline{m}_A$ = 0.9) is connected to a network in which mutualism is a weak selective pressure (coldspot: $\overline{m}_B$ = 0.1). We observed that, in the absence of gene flow, trait matching at equilibrium was more than three-fold higher at the hotspot than at the coldspot (hotspot: $\bar{\tau}_{A,n=100}$ = 0.71 $\pm$ 0.12 vs. coldspot: $\bar{\tau}_{B,n=100}$ = 0.21 $\pm$ 0.007, $\bar{g}$ = 0, Welch two sample t-test: $t_{71.5}$ = 36.33, p < 0.0001; Fig. 2b, c). Interestingly, the effect of gene flow varied with the local selection regime (Fig. 2b, c). At the hotspot, low values of gene flow slightly increased trait matching, but higher values of gene flow ($\bar{g}$ higher than 0.025) decreased trait matching (Likelihood ratio test for linear mixed model: $\chi^2(1)$ = 247.86, p < 0.0001; Fig. 2b; Table S2). In addition, trait matching at the hotspot was higher for high-intimacy mutualisms ($\chi^2(5)$ = 68.98, p < 0.0001) and the loss of trait matching due to gene flow was slightly stronger for high-intimacy mutualisms ($\chi^2(5)$ = 17.22, p = 0.004; Fig. 2b; Table S2). In contrast, gene flow promoted a modest increase in trait matching at the coldspot ($\chi^2(1)$ = 285.02, p < 0.0001; Fig. 2c). Moreover, trait matching at the coldspot was higher for high-intimacy mutualisms ($\chi^2(5)$ = 63.43, p < 0.0001) and the increase in trait matching due to gene flow was slightly stronger for high-intimacy mutualisms ($\chi^2(5)$ = 52.441, p < 0.0001; Fig. 2c; Table S2). Our simulations for other combinations of $\overline{m}_A$ and $\overline{m}_B$ showed that the way gene flow affects trait matching changes gradually as the importance of mutualistic selection increases at the coldspot ($\overline{m}_B$ varying from 0.1 to 0.9; Fig. S5, S6).

In addition to trait matching, we also explored how gene flow and selection mosaics influence the emergence of environmental matching and geographical divergence in traits. We observed that, in the absence of gene flow, the network-level environmental matching ($\bar{\varepsilon}$) at equilibrium was more than two-fold higher in coldspots than in hotspots (coldspot: $\bar{\varepsilon}_{B,n=100}$ = 0.94 $\pm$ 0.02 vs. hotspot: $\bar{\varepsilon}_{A,n=100}$ = 0.37 $\pm$ 0.04, $\bar{g}$ = 0, $\overline{m}_B$ = 0.1, $\overline{m}_A$ = 0.9; Welch two sample t-test: $t_{92.8}$ = 99.26, p < 0.0001). In addition, the environmental matching always decreased with gene flow, irrespective of the selection mosaic (Fig. S7, S8). In agreement with our expectations (Fig. 1), our simulations also indicated that the network-level geographical divergence ($\bar{\delta}$) strongly decreases with gene flow, irrespective of the selection mosaic (Fig. S9).

Effects of network structure on the geographic mosaic of coevolution

Network structure greatly varied among different mutualistic networks (Table S1). Pollinator-plant interactions formed the largest and less connected networks (R = 73 $\pm$ 43.8, C = 0.16 $\pm$ 0.09, mean $\pm$ sd), whereas anemone-fish interactions formed the smallest and more connected networks (R = 8.6 $\pm$ 1.1, C = 0.4 $\pm$ 0.06). Ant-EFN bearing plants interactions formed the most nested networks (standardized *NODF* = 7.3 $\pm$ 7.8), while ant-myrmecophyte interactions formed the most modular networks (standardized Q = 2.3 $\pm$ 0.4). Our PCA identified that 83.1% of the variation in network structure is organized in two structural axes, *PC1* and *PC2* (Fig. 3a; Table S1). *PC1* accounted for 58.5% of all variation in our structural metrics and was strongly correlated with species richness (0.54), degree variance (0.48), and nestedness (0.56; Fig. 3a; Table S3). On the other hand, *PC2* accounted for 24.6% of all variation in our structural metrics and was strongly correlated with connectance (0.68) and modularity (-0.64; Fig. 3a; Table S3).

We explored how network structure, estimated by *PC1* and *PC2* scores, affects the emergence of trait matching in distinct types of selection mosaics. We first focused on how network structure affects trait matching in a selection mosaic composed of two hotspots ($\overline{m}_A = \overline{m}_B$ = 0.9). With no or small gene flow, the *PC1* scores of low-intimacy mutualisms negatively affected the network-level trait matching ($\bar{g}$ = 0: b (regression slope) = -0.022, $F_{1, 51}$ = 8.64, p = 0.005; $\bar{g}$ = 0.01: b = -0.019, $F_{1, 51}$ = 9.98, p = 0.003; Fig. 3b; Table S4). Thus, large, heterogeneous, and nested low-intimacy networks have a low potential of generating trait matching. In contrast, the *PC1* scores of high-intimacy mutualisms did not affect trait matching ($\bar{g}$ = 0: b = 0.016, $F_{1, 17}$ = 0.14, p = 0.71; $\bar{g}$ = 0.01: b = 0.013, $F_{1, 17}$ = 0.13, p = 0.72; Fig. 3b; Table S4). When gene flow was high ($\bar{g}$ = 0.1), *PC1* had no effect on trait matching for both types of mutualisms (low-intimacy: b = -0.003, $F_{1, 51}$ = 1.04, p = 0.31; high-intimacy: b = 0.004, $F_{1, 17}$ = 0.02, p = 0.88; Fig. 3b; Table S4). The *PC2* scores, however, affected the emergence of trait matching in both types of mutualisms and for all three values of gene flow (low-intimacy: $\bar{g}$ = 0: b = -0.033, $F_{1, 51}$ = 10.5, p = 0.002; $\bar{g}$ = 0.01: b = -0.027, $F_{1, 51}$ = 11.24, p = 0.001; $\bar{g}$ = 0.1: b = -0.015, $F_{1, 51}$ = 15.2, p = 0.0002; high-intimacy: $\bar{g}$ = 0: b = -0.022, $F_{1, 17}$ = 5.17, p = 0.04; $\bar{g}$ = 0.01: b = -0.018, $F_{1, 17}$ = 5.6, p = 0.03; $\bar{g}$ = 0.1: b = -0.014, $F_{1, 17}$ = 5.8, p = 0.03; Fig. 3c; Table S4). Therefore, weakly connected and modular networks have a strong potential of generating trait matching.

When the selection mosaic consisted of a hotspot and a coldspot, network structure affected the emergence of trait matching mainly at the hotspot (Fig. S10; Table S4). At the hotspot, *PC1* negatively affected trait matching only in low-intimacy mutualisms and this effect was observed for all values of gene flow (Fig. S10; Table S4). On the other hand, *PC2* negatively affected trait matching in both types of mutualisms with no gene flow, but only in low-intimacy mutualisms with high gene flow (Fig. S10, Table S4). To sum up, our results indicate that network structure affects coevolution when mutualism is an important selective pressure at both localities (i.e. two hotspots), but this effect vanishes with gene flow. In contrast, network structure affects coevolution for variable degrees of gene flow when mutualism is an important selective pressure at one locality but is unimportant at the other locality (i.e. one hotspot and one coldspot; Fig. S10).

In order to have a detailed picture of the effects of network structure for the whole parameter space, we performed an additional set of simulations in which we used many combinations of $\bar{g}$, $\overline{m}_A$, and $\overline{m}_B$ for one ant-myrmecophyte and one pollinator-plant network with contrasting structures (networks 29 and 65 in Table S1; Fig. 3a). These results confirmed that high-intimacy mutualisms promote the emergence of higher values of trait matching and are weakly affected by gene flow (Fig. S11, S12). On the other hand, low-intimacy mutualisms generate lower values of trait matching in general, but are more affected by gene flow (Fig. S11, S12).

Coevolutionary effects of habitat fragmentation

In our last set of simulations, we used our coevolution model to simulate habitat fragmentation that would result in the disruption of gene flow between two hotspots ($\overline{m}_A = \overline{m}_B = 0.9$). As expected from our previous analyses, species lost their trait matching with mutualistic partners when gene flow between the two hotspots was removed ($\bar{g} = 0.1$: $\bar{\tau}_{A,n=100} = 0.85 \pm 0.05$; $\bar{g} = 0$: $\bar{\tau}_{A,n=100} = 0.79 \pm 0.06$; Fig. 4a). Our linear mixed models confirmed that trait matching decreases with the loss of gene flow (Likelihood ratio test: $\chi^2(1) = 141.8$, $p < 0.0001$), that trait matching is always higher for high-intimacy mutualisms ($\chi^2(5) = 69.89$, $p < 0.0001$), and that the effect of losing gene flow is stronger for low-intimacy mutualisms ($\chi^2(5) = 37.64$, $p < 0.0001$; Fig. 4b). Interestingly, however, the final values of trait matching in these simulations

were higher than the values observed in our previous simulations, especially for low-intimacy mutualisms (Fig. 2a, 4b; $\bar{g}$ = 0). This result indicates that species in fragmented landscapes may attain higher values of trait matching if their initial trait values are highly matched (e.g. traits at equilibrium for $\bar{g}$ = 0.1) than if their initial trait values are poorly matched (e.g. trait values start at the environmental optimum: $\bar{z}_{i,A}(0) = \theta_{i,A}$ and $\bar{z}_{i,B}(0) = \theta_{i,B}$; Fig. S13).

In parallel with the loss of coadaptations between mutualistic partners following habitat fragmentation, species greatly improved their environmental matching ($\bar{g}$ = 0.1: $\bar{\varepsilon}_A$ = 0.08 $\pm$ 0.009; $\bar{g}$ = 0: $\bar{\varepsilon}_A$ = 0.31 $\pm$ 0.03; Fig. 4a). Our linear mixed models showed that environmental matching increases with the loss of gene flow ($\chi^2(1)$ = 467.7, p < 0.0001), that environmental matching is lower for low-intimacy mutualisms ($\chi^2(1)$ = 32, p < 0.0001), and that the effect of losing gene flow is more pronounced in high-intimacy mutualisms ($\chi^2(1)$ = 124.4, p < 0.0001; Fig. 4c).

Discussion

The geographical and ecological complexity of coevolution poses a challenge to our understanding of the evolution of interacting species. By simulating coevolution with information on the structure of empirical mutualistic networks we were able to identify three fundamental aspects of how species evolve when embedded in ecological assemblages across simple landscapes. First, gene flow affects the evolutionary outcomes of selection between mutualistic partners and may favor the emergence of trait matching depending on the geographic selection mosaic. Second, the network structure of different mutualisms affects coevolution in distinct ways, but the effect of network structure may vanish when gene flow fuels the emergence of trait matching. Third, habitat fragmentation resulting in the disruption of gene flow should reduce the coadaptations between mutualistic partners while promoting adaptations of species to their local environment.

The influence of gene flow on the evolution of populations is a key aspect of evolutionary theory (Slatkin 1987; Lenormand 2002). In the context of the GMTC, gene flow is a central process affecting patterns of trait matching in pairs of interacting populations (Anderson & Johnson 2008; Yoder *et al.* 2013). Mathematical models show that some of the phenotypic patterns predicted by the GMTC result from

complex interplays between gene flow and selection mosaics (Nuismer *et al.* 1999; Gomulkiewicz *et al.* 2000; Gibert *et al.* 2013). In networks of interacting species, our simulations indicate that gene flow may either increase or decrease trait matching between interacting populations depending on the selection mosaic. When gene flow connects two networks under strong mutualistic selection (i.e. two hotspots), gene flow has a counterintuitive effect of favoring trait matching between mutualistic partners. We suggest that such an effect is a consequence of how gene flow affects the outcome of selection exerted by mutualistic partners and selection exerted by the environment (i.e. abiotic factors and other ecological interactions). When gene flow connects two hotspots with different environmental adaptive peaks (i.e. $\theta_{i,A} < \theta_{i,B}$ for every species *i*) the effects of environmental selection are cancelled out, leading to a loss of adaptation to the local environment (Fig. S7, S8) and to a geographical homogenization in species traits (Fig. S9). The mismatch with the local environment in turn favors selection for tight coadaptations between mutualistic partners at the landscape level. It is known that traits adapted to certain ecological interactions may reduce survival, reproduction, or performance with respect to other selective pressures (Fine *et al.* 2006; Ågren *et al.* 2013). In these circumstances, gene flow could act to fuel coadaptations between interacting populations, providing a mechanism for how traits that mediate ecological interactions become fixed at the species level (Thompson 2005). Our results indicate that such an effect could be amplified when networks of interacting species are connected by gene flow and form a single multilayer network. In fact, recent studies on multilayer networks indicate that linking two or more networks together may substantially alter the ecological dynamics (Kéfi *et al.* 2016) or other kinds of dynamics such as disease spreading (Boccaletti *et al.* 2014).

In contrast to two linked hotspots, we observed that gene flow has an opposite effect on trait matching if a network at a hotspot is connected to a network under weak mutualistic selection (i.e. a coldspot). Because populations at the coldspot are locked to their local environmental adaptive peaks, populations at the hotspot receive a constant input of maladapted phenotypes from the coldspot, which leads to trait mismatching at the hotspot. In this sense, our study provides additional evidence that maladaptation may emerge through the combination of gene flow and selection mosaics (Gomulkiewicz *et al.* 2000; Thompson 2005; Hanifin *et al.* 2008).

Experimental coevolution between bacteria and phage shows that migration between a hotspot and a coldspot promotes coevolution at the coldspot, but inhibits coevolution at the hotspot (Vogwill *et al.* 2009). Our results indicate that this phenomenon also occurs in mutualistic networks, suggesting that contrasting selective pressures across localities may also be important for the evolutionary dynamics of whole communities (Urban *et al.* 2008).

Multispecies mutualistic systems are not randomly organized, but instead show typical architectures that may affect ecological and evolutionary processes (Bascompte & Jordano 2014). Our results show that the network structure of high-intimacy mutualisms promote the emergence of higher levels of trait matching between mutualistic partners than the network structure of low-intimacy mutualisms. Networks of intimate mutualisms are typically characterized by a small number of species grouped in semi-isolated modules (Ricciardi *et al.* 2010; Dáttilo *et al.* 2013b; this study). Previous theoretical studies suggest that the compartmentalized nature of these networks may promote reciprocal evolution (Guimarães *et al.* 2007a) and may emerge as a consequence of trait matching (Andreazzi *et al.* 2017). These results are in agreement with the impressive degree of specificity observed in interactions such as ants that protect myrmecophytes, in which interacting individuals show very tight morphological, behavioral, and biochemical matches (Brouat *et al.* 2001; Orona-Tamayo *et al.* 2013). In fact, we found that the least connected structure of networks of protective ants and their host plants (Fonseca & Ganade 1996; Blüthgen *et al.* 2007; Guimarães *et al.* 2007a) favors the coevolutionary emergence of trait matching through reciprocal specialization in our numerical simulations.

In contrast to high-intimacy mutualisms, the emergence of elevated trait matching in low-intimacy mutualisms is contingent upon gene flow between hotspots. Our model suggests that the network structure of low-intimacy mutualisms amplifies the effect of gene flow of cancelling out opposing environmental selective pressures, allowing the emergence of strong trait matching. A collateral effect of this mechanism, however, is that gene flow blurs the effect of the network structure of low-intimacy mutualisms (Fig. 3b, c). Low-intimacy mutualisms between free-living species are characterized by species-rich networks with a core of generalist species (Bascompte *et al.* 2003; Guimarães *et al.* 2006, 2007b; this study). Theoretical work on evolution in mutualistic and antagonistic networks indicates that these generalist species may

fuel coevolution and promote trait convergence and trait matching in the network (Guimarães *et al.* 2011; Andreazzi *et al.* 2017). Here, we report a similar effect of the network structure of mutualisms among free-living species, which is mediated by gene flow between two hotspots. On the other hand, when a hotspot is connected to a coldspot, gene flow does not promote trait matching at the hotspot and, as a consequence, does not blur the effect of the network structure on trait matching (Fig. S10). These results suggest that network structure plays a prominent role in coevolution whenever there are pairs of species with poorly matched traits, which fuel coevolutionary change through their structural role in the network (Guimarães *et al.* 2011; Andreazzi *et al.* 2017). Because hotspots are often surrounded by multiple coldspots (Thompson & Cunningham 2002; Hanifin *et al.* 2008), we predict that network structure will usually be a central component of the coevolutionary dynamics of species-rich mutualisms.

If gene flow influences the outcome of coevolution in mutualistic networks, habitat fragmentation may affect coevolution through the disruption of gene flow. Indeed, our simulations of habitat fragmentation in two hotspots show that the disruption of gene flow would lead to the reduction of trait matching between mutualistic partners, especially in mutualisms with low interaction intimacy. There is empirical evidence that human impact may fuel evolutionary changes in mutualisms by changing the species composition of interacting partners (Toby Kiers *et al.* 2010; Galetti *et al.* 2013). Here, we suggest that habitat fragmentation may have an insidious effect on the organization of mutualistic interactions by changing patterns of coadaptation in species-rich networks. Interestingly, however, we found that the emergence of trait matching in the absence of gene flow depended on the initial trait values (Fig. S13). Biologically, this effect of the initial condition means that species in fragmented areas would still show signs of their coevolved traits when gene flow was present long after the fragmentation event. Therefore, we provide evidence that past coevolutionary events may constrain subsequent evolution in species-rich mutualisms. Although species lose their adaptations to mutualistic partners, we found that species increase their adaptations to the local environment with the loss of gene flow. This effect was stronger for intimate mutualisms, meaning that habitat fragmentation has a stronger potential for population differentiation in mutualisms that are organized as small networks with semi-isolated groups of interacting species.

Thus, the divergence in traits of isolated populations may be an additional consequence of fragmentation for the structure and dynamics of high-intimacy mutualistic networks (Emer, 2013).

In this study, we investigated how fundamental processes of the GMTC affect coevolution in different kinds of mutualistic networks. Although we explored simple simulation scenarios of a mathematical model with many underlying assumptions, we think that our analyses represent a first step to unravel the complexity of the coevolutionary process in multispecies systems across space. Because the species composition of communities and network structure often vary across space (Dáttilo *et al.* 2013a; Carstensen *et al.* 2014; Gilarranz *et al.* 2015; Trojelsgaard *et al.* 2015), a next step is to use datasets with spatial variation and tools from multilayer networks to explore coevolutionary dynamics. Ultimately, our approach allowed us to strengthen the connections between two research topics in coevolution that are inseparable: multispecies coevolution and the geographic mosaic of coevolution (Thompson 2005; Bascompte & Jordano 2014; Carmona *et al.* 2015). In particular, we provide a theoretical basis to understand how coadaptations should evolve when communities contain dozens of interacting species. We show that a complex interplay between gene flow, the geographic structure of selection, and the network organization of mutualisms shapes trait matching in mutualistic assemblages. Our results therefore provide clear predictions of how the geographic mosaic of coevolution shapes species-rich interactions often considered diffuse. Such predictions of the evolutionary trajectory of whole communities are key to our understanding of the impacts of widespread modification and fragmentation of natural landscapes driven by human action.

Acknowledgements

We thank P. I. Prado, R. Vicente, J. N. Thompson, R. Cogni, P. Jordano, A. P. Assis, I. B. Barros, M. P. Gaiarsa, G. Garcia, M. S. Leite, P. Lemos-Costa, D. Melo, L. Nascimento, and G. S. Requena for valuable suggestions and for discussions regarding this work. We also thank the researchers that kindly provided their empirical datasets of ecological interactions. The São Paulo Research Foundation (FAPESP) provided financial support to LPM (grant 2015/12956-7) and PRG (grants 2009/54422-9 and 2016/20739-9).

The National Council for Scientific and Technological Development (CNPq) provided financial support to LPM (grant 131177/2015-0).

References

1. Ågren, J., Hellström, F., Toräng, P. & Ehrlén, J. (2013). Mutualists and antagonists drive among-population variation in selection and evolution of floral display in a perennial herb. *Proc. Natl. Acad. Sci.*, 110, 18202–18207

2. Almeida-Neto, M., Guimarães, P., Guimarães, P.R., Loyola, R.D. & Ulrich, W. (2008). A consistent metric for nestedness analysis in ecological systems: reconciling concept and measurement. *Oikos*, 117, 1227–1239

3. Anderson, B. & Johnson, S.D. (2008). The Geographical Mosaic of Coevolution in a Plant-Pollinator Mutualism. *Evolution*, 62, 220–225

4. Andreazzi, C.S., Thompson, J.N. & Guimarães Jr, P.R. (2017). Network Structure and Selection Asymmetry Drive Coevolution in Species-Rich Antagonistic Interactions. *Am. Nat.*, 190

5. Barber, M.J. (2007). Modularity and community detection in bipartite networks. *Phys. Rev. E*, 76, 66102

6. Bascompte, J. & Jordano, P. (2014). *Mutualistic Networks*. Princeton University Press, Princeton, New Jersey

7. Bascompte, J., Jordano, P., Melián, C.J. & Olesen, J.M. (2003). The nested assembly of plant–animal mutualistic networks. *Proc. Natl. Acad. Sci.*, 100, 9383–9387

8. Bates, D., Mächler, M., Bolker, B. & Walker, S. (2015). Fitting Linear Mixed-Effects Models using lme4. *J. Stat. Softw.*, 67, 1–48

9. Benkman, C.W., Parchman, T.L., Favis, A. & Siepielski, A.M. (2003). Reciprocal selection causes a coevolutionary arms race between crossbills and lodgepole pine. *Am. Nat.*, 162, 182–94

10. Benkman, C.W., Smith, J.W., Maier, M., Hansen, L. & Talluto, M. V. (2013). Consistency and variation in phenotypic selection exerted by a community of seed predators. *Evolution*, 67, 157–169

11. Blüthgen, N., Menzel, F., Hovestadt, T., Fiala, B. & Blüthgen, N. (2007). Specialization, Constraints, and Conflicting Interests in Mutualistic Networks. *Curr. Biol.*, 17, 341–346

12. Boccaletti, S., Bianconi, G., Criado, R., del Genio, C.I., Gómez-Gardeñes, J., Romance, M., *et al.* (2014). The structure and dynamics of multilayer networks. *Phys. Rep.*, 544, 1–122

13. Brouat, C., Garcia, N., Andary, C. & McKey, D. (2001). Plant lock and ant key: pairwise coevolution of an exclusion filter in an ant-plant mutualism. *Proc. R. Soc. B Biol. Sci.*, 268, 2131–2141

14. Carmona, D., Fitzpatrick, C.R. & Johnson, M.T.J. (2015). Fifty years of co-evolution and beyond: integrating co-evolution from molecules to species. *Mol. Ecol.*, 24, 1–15

15. Carstensen, D.W., Sabatino, M., Trøjelsgaard, K. & Morellato, L.P.C. (2014). Beta diversity of plant-pollinator networks and the spatial turnover of pairwise interactions. *PLoS One*, 9, 1–7

16. Cheptou, P.-O., Hargreaves, A.L., Bonte, D. & Jacquemyn, H. (2017). Adaptation to fragmentation: evolutionary dynamics driven by human influences. *Philos. Trans. R. Soc. B Biol. Sci.*, 372, 20160037

17. Dáttilo, W., Guimarães, P.R. & Izzo, T.J. (2013a). Spatial structure of ant-plant mutualistic networks. *Oikos*, 122, 1643–1648

18. Dáttilo, W., Izzo, T.J., Vasconcelos, H.L. & Rico-Gray, V. (2013b). Strength of the modular pattern in Amazonian symbiotic ant–plant networks. *Arthropod. Plant. Interact.*, 7, 455–461

19. Dormann, C.F., Gruber, B. & Fründ, J. (2008). Introducing the bipartite Package: Analysing Ecological Networks. *R News*, 8, 8–11

20. Fine, P.V.A., Miller, Z.J., Mesones, I., Irazuzta, S., Appel, H.M., Stevens, M.H.H., *et al.* (2006). The Growth–Defense Trade-Off and Habitat Specialization By Plants in Amazonian Forests. *Ecology*, 87, S150–S162

21. Fitzpatrick, S.W., Gerberich, J.C., Kronenberger, J.A., Angeloni, L.M. & Funk, W.C. (2015). Locally adapted traits maintained in the face of high gene flow. *Ecol. Lett.*, 18, 37–43

22. Fonseca, C.R. & Ganade, G. (1996). Asymmetries, compartments and null interactions in an Amazonian ant-plant community. *J. Anim. Ecol.*, 65, 339–347

23. Fontaine, C., Guimarães, P.R., Kéfi, S., Loeuille, N., Memmott, J., van der Putten, W.H., *et al.* (2011). The ecological and evolutionary implications of merging different types of networks. *Ecol. Lett.*, 14, 1170–1181

24. Fortuna, M.A., Stouffer, D.B., Olesen, J.M., Jordano, P., Mouillot, D., Krasnov, B.R., *et al.* (2010). Nestedness versus modularity in ecological networks: two sides of the same coin? *J. Anim. Ecol.*, 79, 811–817

25. Frederickson, M.E. & Gordon, D.M. (2009). The Intertwined Population Biology of Two Amazonian Myrmecophytes and Their Symbiotic Ants. *Ecology*, 90, 1595–1607

26. Galetti, M., Guevara, R., Cortes, M.C., Fadini, R., Von Matter, S., Leite, A.B., *et al.*

(2013). Functional Extinction of Birds Drives Rapid Evolutionary Changes in Seed Size. *Science*, 340, 1086–1090

27. Gandon, S. (2002). Local adaptation and the geometry of host-parasite coevolution. *Ecol. Lett.*, 5, 246–256

28. Gervasi, D.D.L. & Schiestl, F.P. (2017). Real-time divergent evolution in plants driven by pollinators. *Nat. Commun.*, 8, 14691

29. Gibert, J.P., Pires, M.M., Thompson, J.N. & Guimarães, P.R. (2013). The spatial structure of antagonistic species affects coevolution in predictable ways. *Am. Nat.*, 182, 578–91

30. Gilarranz, L.J., Sabatino, M., Aizen, M.A. & Bascompte, J. (2015). Hot spots of mutualistic networks. *J. Anim. Ecol.*, 84, 407–413

31. Gómez, J.M., Perfectti, F., Bosch, J. & Camacho, J.P.M. (2009). A geographic selection mosaic in a generalized plant-pollinator-herbivore system. *Ecol. Monogr.*, 79, 245–263

32. Gomulkiewicz, R., Thompson, J.N., Holt, R.D., Nuismer, S.L. & Hochberg, M.E. (2000). Hot Spots, Cold Spots, and the Geographic Mosaic Theory of Coevolution. *Am. Nat.*, 156, 156–174

33. Grant, P.R. & Grant, B.R. (2006). Evolution of Character Displacement in Darwin's Finches. *Science*, 313, 224–226

34. Guimarães, P.R., Jordano, P. & Thompson, J.N. (2011). Evolution and coevolution in mutualistic networks. *Ecol. Lett.*, 14, 877–885

35. Guimarães, P.R., Rico-Gray, V., Oliveira, P.S., Izzo, T.J., dos Reis, S.F. & Thompson, J.N. (2007a). Interaction Intimacy Affects Structure and Coevolutionary Dynamics in Mutualistic Networks. *Curr. Biol.*, 17, 1797–1803

36. Guimarães, P.R., Rico-Gray, V., dos Reis, S.F. & Thompson, J.N. (2006). Asymmetries in specialization in ant-plant mutualistic networks. *Proc. R. Soc. B Biol. Sci.*, 273, 2041–2047

37. Guimarães, P.R., Sazima, C., dos Reis, S.F. & Sazima, I. (2007b). The nested structure of marine cleaning symbiosis: is it like flowers and bees? *Biol. Lett.*, 3, 51–54

38. Hagen, M., W. Daniel Kissling, Rasmussen, C., Aguiar, M.A.M. de, Brown, L., Carstensen, D.W., *et al.* (2012). Biodiversity, species interactions and ecological networks in a fragmented world. *Adv. Ecol. Res.*, 46, 89–120

39. Hanifin, C.T., Brodie, E.D. & Brodie, E.D. (2008). Phenotypic mismatches reveal escape from arms-race coevolution. *PLoS Biol.*, 6, 0471–0482

40. Hendry, A.P. & Taylor, E.B. (2004). How Much of the Variation in Adaptive Divergence Can Be Explained By Gene Flow? An Evaluation Using Lake-Stream

Stickleback Pairs. *Evolution*, 58, 2319–2331

41. Ings, T.C., Montoya, J.M., Bascompte, J., Blüthgen, N., Brown, L., Dormann, C.F., *et al.* (2009). Ecological networks — Beyond food webs. *J. Anim. Ecol.*, 78, 253–269

42. Iwao, K. & Rausher, M.D. (1997). Evolution of plant resistance to multiple herbivores: quantifying diffuse coevolution. *Am. Nat.*, 149, 316–335

43. Jordano, P. (1987). Patterns of mutualistic interactions in pollination and seed dispersal: connectance, dependence asymmetries, and coevolution. *Am. Nat.*, 129, 657–677

44. Kéfi, S., Miele, V., Wieters, E.A., Navarrete, S.A. & Berlow, E.L. (2016). How Structured Is the Entangled Bank? The Surprisingly Simple Organization of Multiplex Ecological Networks Leads to Increased Persistence and Resilience. *PLoS Biol.*, 14, 1–21

45. Krebs, C.J., Boutin, S., Boonstra, R., Sinclair, A.R.E., Smith, J.N.M., Dale, M.R.T., *et al.* (1995). Impact of Food and Predation on the Snowshoe Hare Cycle. *Science*, 269, 1112–1115

46. Lande, R. (1976). Natural selection and random genetic drift in phenotypic evolution. *Evolution*, 30, 314–334

47. Lenormand, T. (2002). Gene flow and the limits to natural selection. *Trends Ecol. Evol.*, 17, 183–189

48. Loeuille, N. (2010). Influence of evolution on the stability of ecological communities. *Ecol. Lett.*, 13, 1536–1545

49. Marquitti, F.M.D., Guimarães, P.R., Pires, M.M. & Bittencourt, L.F. (2014). MODULAR: Software for the Autonomous Computation of Modularity in Large Network Sets. *Ecography*, 37, 221–224

50. Newman, E., Manning, J. & Anderson, B. (2014). Matching floral and pollinator traits through guild convergence and pollinator ecotype formation. *Ann. Bot.*, 113, 373–384

51. Nuismer, S.L., Gomulkiewicz, R. & Ridenhour, B.J. (2010). When Is Correlation Coevolution? *Am. Nat.*, 175, 525–537

52. Nuismer, S.L., Jordano, P. & Bascompte, J. (2013). Coevolution and the architecture of mutualistic networks. *Evolution*, 67, 338–354

53. Nuismer, S.L., Thompson, J.N. & Gomulkiewicz, R. (1999). Gene flow and geographically structured coevolution. *Proc. R. Soc. B*, 266, 605–609

54. Olesen, J.M., Bascompte, J., Dupont, Y.L. & Jordano, P. (2007). The modularity of pollination networks. *Proc. Natl. Acad. Sci.*, 104, 19891–19896

55. Ollerton, J. (2006). “Biological Barter”: Patterns of Specialization Compared across Different Mutualisms. In: *Plant–pollinator interactions: from specialization to generalization* (eds. Waser, N.M. & Ollerton, J.). The University of Chicago Press, Chicago, pp. 411–435

56. Orona-Tamayo, D., Wielsch, N., Blanco-Labra, A., Svatos, A., Farías-Rodríguez, R. & Heil, M. (2013). Exclusive rewards in mutualisms: Ant proteases and plant protease inhibitors create a lock-key system to protect *Acacia* food bodies from exploitation. *Mol. Ecol.*, 22, 4087–4100

57. Piculell, B.J., Hoeksema, J.D. & Thompson, J.N. (2008). Interactions of biotic and abiotic environmental factors on an ectomycorrhizal symbiosis, and the potential for selection mosaics. *BMC Biol.*, 6

58. R Core Team. (2016). R: A language and environment for statistical computing

59. Raimundo, R.L.G., Gibert, J.P., Hembry, D.H. & Guimarães, P.R. (2014). Conflicting Selection in the Course of Adaptive Diversification: The Interplay between Mutualism and Intraspecific Competition. *Am. Nat.*, 183, 363–375

60. Ramírez, S.R., Eltz, T., Fujiwara, M.K., Gerlach, G., Goldman-Huertas, B., Tsutsui, N.D., *et al.* (2011). Asynchronous diversification in a specialized plant-pollinator mutualism. *Science*, 333, 1742–1746

61. Ricciardi, F., Boyer, M. & Ollerton, J. (2010). Assemblage and interaction structure of the anemonefish-anemone mutualism across the Manado region of Sulawesi, Indonesia. *Environ. Biol. Fishes*, 87, 333–347

62. Rudgers, J.A. & Strauss, S.Y. (2004). A selection mosaic in the facultative mutualism between ants and wild cotton. *Proc. R. Soc. Lond. B*, 271, 2481–2488

63. Santamaría, L. & Rodríguez-Gironés, M.A. (2007). Linkage Rules for Plant–Pollinator Networks: Trait Complementarity or Exploitation Barriers? *PLOS Biol.*, 5, 0354–0362

64. Silvestro, D., Antonelli, A., Salamin, N. & Quental, T.B. (2015). The role of clade competition in the diversification of North American canids. *Proc. Natl. Acad. Sci.*, 112, 8684–8689

65. Slatkin, M. (1987). Gene flow and the geographic structure of natural populations. *Science*, 236, 787–792

66. Strauss, S.Y. & Irwin, R.E. (2004). Ecological and Evolutionary Consequences of Multispecies Plant-Animal Interactions. *Annu. Rev. Ecol. Evol. Syst.*, 35, 435–466

67. Thompson, J.N. (2005). *The geographic mosaic of coevolution*. The University of Chicago Press, Chicago

68. Thompson, J.N. (2009). The Coevolving Web of Life (American Society of Naturalists Presidential Address). *Am. Nat.*, 173, 125–140

69. Thompson, J.N. & Cunningham, B.M. (2002). Geographic structure and dynamics of coevolutionary selection. *Nature*, 171, 1997–2000

70. Toby Kiers, E., Palmer, T.M., Ives, A.R., Bruno, J.F. & Bronstein, J.L. (2010). Mutualisms in a changing world: An evolutionary perspective. *Ecol. Lett.*, 13, 1459–1474

71. Trojelsgaard, K., Jordano, P., Carstensen, D.W. & Olesen, J.M. (2015). Geographical variation in mutualistic networks: similarity, turnover and partner fidelity. *Proc. R. Soc. B Biol. Sci.*, 282, 20142925

72. Urban, M.C., Leibold, M.A., Amarasekare, P., De Meester, L., Gomulkiewicz, R., Hochberg, M.E., *et al.* (2008). The evolutionary ecology of metacommunities. *Trends Ecol. Evol.*, 23, 311–317

73. Vogwill, T., Fenton, A., Buckling, A., Hochberg, M.E. & Brockhurst, M.A. (2009). Source Populations Act as Coevolutionary Pacemakers in Experimental Selection Mosaics Containing Hotspots and Coldspots. *Am. Nat.*, 173, E171–E176

74. White, J.W., Rassweiler, A., Samhouri, J.F., Stier, A.C. & White, C. (2014). Ecologists should not use statistical significance tests to interpret simulation model results. *Oikos*, 123, 385–388

75. Yoder, J.B., Smith, C.I., Rowley, D.J., Flatz, R., Godsoe, W., Drummond, C., *et al.* (2013). Effects of gene flow on phenotype matching between two varieties of Joshua tree (*Yucca brevifolia*; Agavaceae) and their pollinators. *J. Evol. Biol.*, 26, 1220–1233

Figures

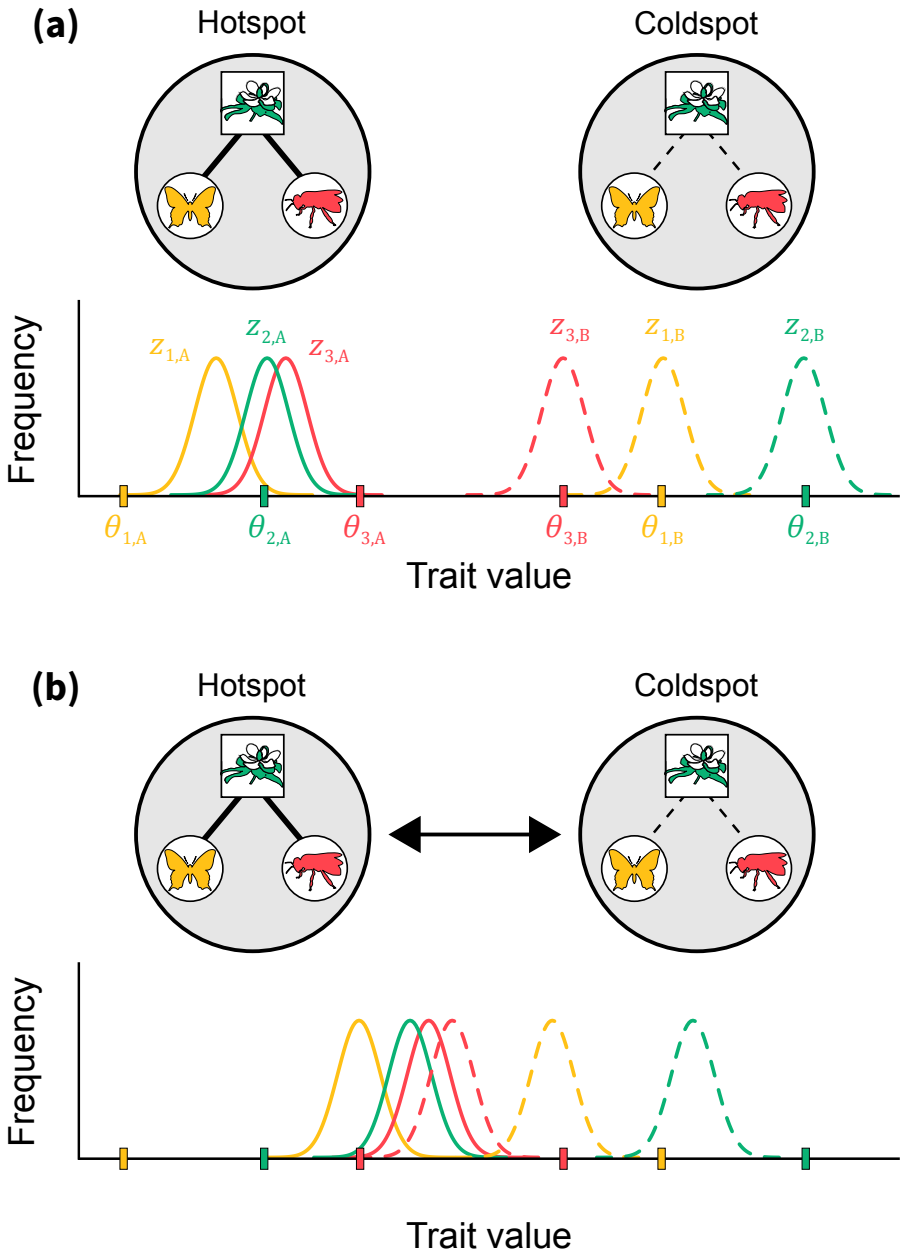

Figure 1. Hypothesized effects of selection mosaics and gene flow on the coevolution of species embedded in a mutualistic network. Each population *i* at a given locality (*A* or *B*) is associated with a distribution of a trait that mediates the mutualism ($z_{i,A}$, $z_{i,B}$) and a trait value favored by the local environment ($\theta_{i,A}$, $\theta_{i,B}$). At the hotspot (locality *A*, left), there is strong selection imposed by the mutualism between two pollinators (yellow and red) and one plant species (green) and the environment selects for small trait values ($\theta_{i,A}$). At the coldspot (locality *B*, right), the environment exerts a stronger selection than mutualism and selects for large trait values ($\theta_{i,B}$). When both localities are isolated (a), we expect that coevolution should generate a higher trait matching between interacting populations at the hotspot than at the coldspot. At the coldspot,

each population should become well adapted to its local environment. When both localities are connected by gene flow (b), we expect a reduction in the geographical divergence of traits. However, the effects of gene flow on the emergence of trait matching at each locality are hard to predict and define a current major challenge for coevolutionary research.

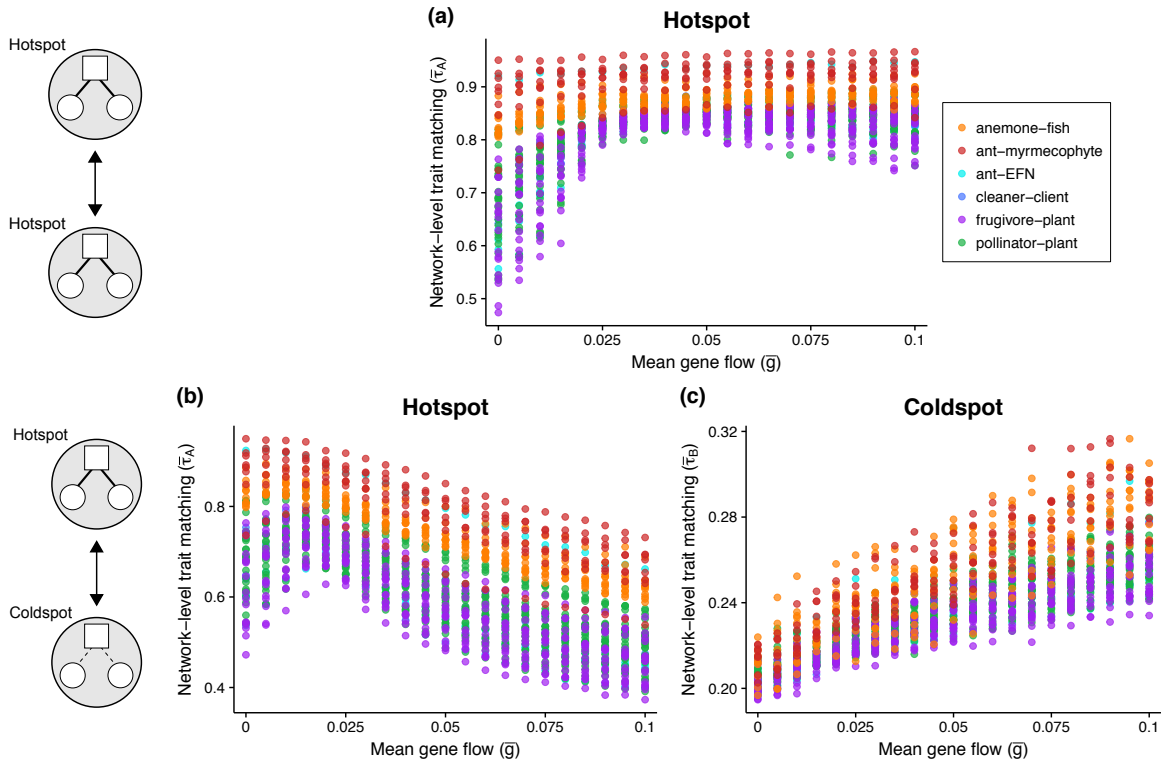

Figure 2. The effects of gene flow and selection mosaics on coevolution in mutualistic networks. For a hotspot connected to another hotspot (a), gene flow increased the network-level trait matching ($\bar{\tau}_A$) generated by coevolution. High-intimacy mutualisms (orange and red points) attained higher values of trait matching and were less affected by gene flow than low-intimacy mutualisms (blue, purple, and green points). For a hotspot connected to a coldspot (b), low values of gene flow slightly increased trait matching, but high values of gene flow ($\bar{g}$ > 0.025) decreased trait matching. For a coldspot connected to a hotspot (c), gene flow promoted a modest increase in trait matching. In all plots, each point corresponds to the mean of the network-level trait matching for 100 simulations for a given network ($\bar{\tau}_{A,n=100}$ or $\bar{\tau}_{B,n=100}$). The mean importance of mutualistic selection was $\bar{m}_A$ = 0.9 at the hotspot and $\bar{m}_B$ = 0.1 at the coldspot.

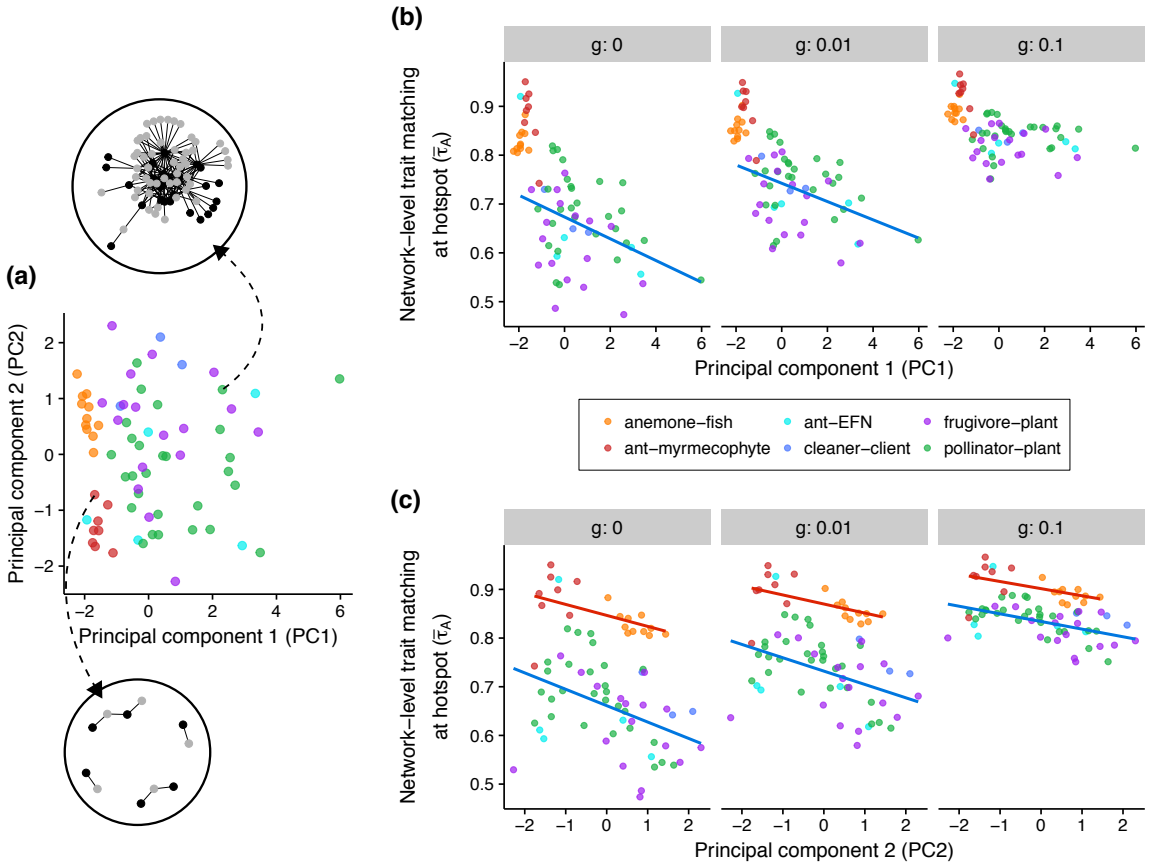

Figure 3. Mutualistic network structure mediates the effects of gene flow on coevolution in two connected hotspots. Our two principal components (*PC1* and *PC2*) explained 83.1% of the variation of network structure in our dataset (a). *PC1* was positively correlated with species richness and nestedness and *PC2* was positively correlated with connectance and negatively correlated with modularity. In one extreme we had large and nested networks, such as a network with 25 pollinators (black nodes) and 51 plants (grey nodes) from a semi-arid region in Brazil (*PC1* = 2.31, *PC2* = 1.16; network 29 in Table S1). In the other extreme we had small and modular networks, such as a network with 6 protective ants (black nodes) and 5 host plants (grey nodes) from the Brazilian Amazon (*PC1* = -1.68, *PC2* = -0.72; network 65 in Table S1). (b) *PC1* only affected the emergence of trait matching in two isolated ($\bar{g}$ = 0) or weakly connected ($\bar{g}$ = 0.01) hotspots and for low-intimacy mutualisms (blue, purple, and green points; lines show significant regressions). On the other hand (c), *PC2* affected the emergence of trait matching for all values of gene flow and for both types of mutualisms (blue lines: low-intimacy mutualisms; red lines and orange and red points: high-intimacy mutualisms). However, the importance of network structure greatly reduced when gene flow favored trait matching (b-c; $\bar{g}$ = 0.1). In (b-c) each point corresponds to the mean of the network-level trait matching for 100 simulations for a given network ($\bar{\tau}_{A,n=100}$). The mean importance of mutualistic selection was $\overline{m}_A$ = $\overline{m}_B$ = 0.9.

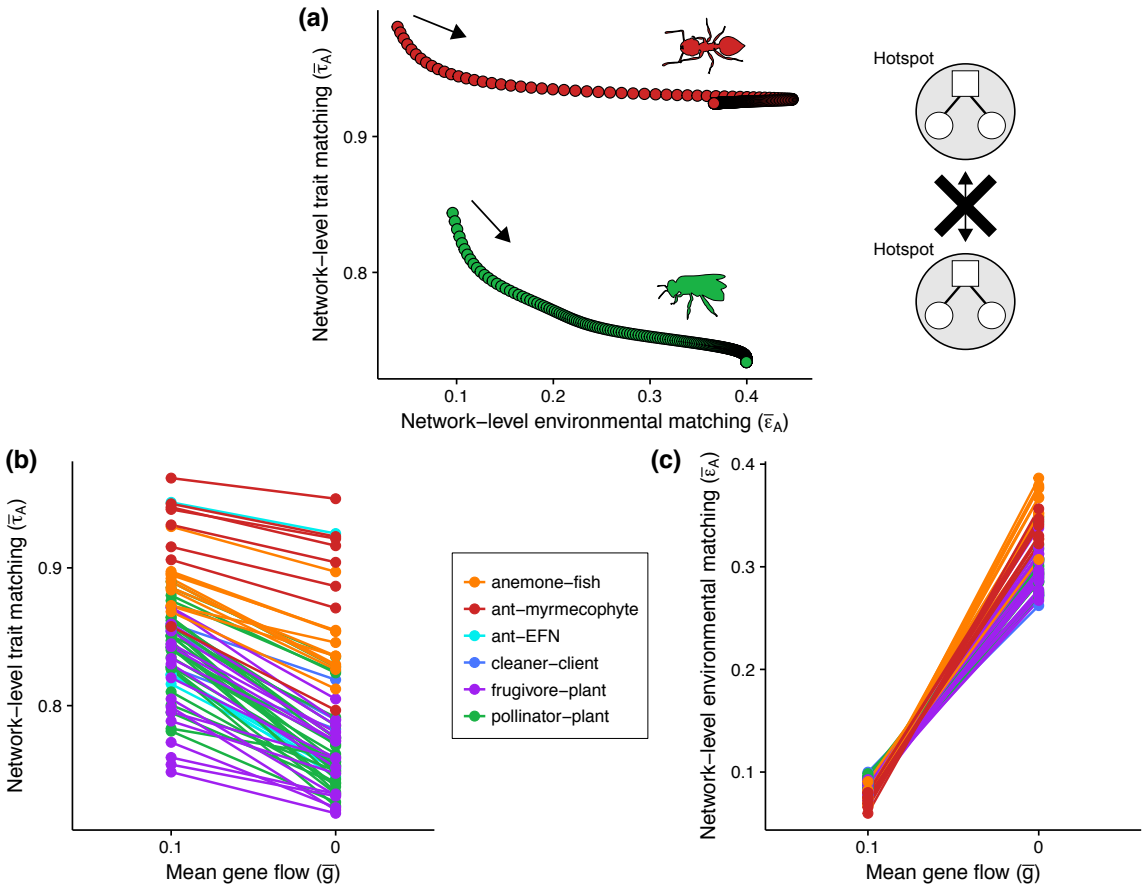

Figure 4. Habitat fragmentation and disruption of gene flow may profoundly impact coevolution in mutualistic networks. In a given simulation in which gene flow between two hotspots was removed (a), species lost their coadaptations with mutualistic partners (i.e. trait matching), but increased their adaptations to the local environment (i.e. environmental matching). In (a) each point represents the network-level trait matching ($\bar{\tau}_A$) and environmental matching ($\bar{\varepsilon}_A$) in a given time step and arrows point in the direction of time evolution (red: ant-myrmecophyte network 65 in Table S1; green: pollinator-plant network 29 in Table S1). (b) High-intimacy mutualisms (orange and red points) generated higher values of trait matching, but the reduction in trait matching following the disruption of gene flow was more pronounced in low-intimacy mutualisms (blue, purple, and green points). However (c), the increase in environmental matching following the disruption of gene flow was stronger for high-intimacy mutualisms. Each point in (b-c) corresponds to the mean of the network-level metric for 100 simulations for a given network ($\bar{\tau}_{A,n=100}$ or $\bar{\varepsilon}_{A,n=100}$) and lines connect the same network. The mean importance of mutualistic selection in these simulations was $\bar{m}_A = \bar{m}_B = 0.9$.

Supporting Information

Gene flow and selection mosaics shape coevolution in mutualistic networks

Lucas P. Medeiros & Paulo R. Guimarães Jr.

Network structure metrics

Here we describe how we calculated each of our five metrics of network structure: (i) species richness (R), (ii) degree variance (σ_k^2), (iii) connectance (C), (iv) nestedness ($NODF$), and (v) modularity (Q). We used these metrics to quantify the organization of interactions of our 72 empirical mutualistic networks, which were represented as binary bipartite adjacency matrices. Each network is composed of two distinct sets of species (e.g. pollinators and plants) and interactions only occur between species of different sets. In matrix **A**, one set is positioned in the rows and the other in the columns and an element a_{ij} = 1 if species i and j are mutualistic partners or a_{ij} = 0 if they are not. We used this information to parameterize the simulations of our coevolution model with the additional restriction that a_{ij} = 0 if species i and j belong to different sets.

If the first set has R_1 species (i.e. number of rows in **A**) and the second set has R_2 species (i.e. number of columns in **A**), then species richness is calculated as $R = R_1 + R_2$. The number of interactions or degree of species i present in the first set is quantified as $k_i = \sum_j^{R_2} a_{ij}$ and the degree of species j present in the second group as $k_j = \sum_i^{R_1} a_{ij}$. The degree variance is simply the variance of the degree values (k_i) of all species in the network. Defining the total number of interactions in the network as $I = \sum_i^{R_1} \sum_j^{R_2} a_{ij}$, network connectance may be calculated as $C = \frac{I}{R_1 R_2}$ and represents the proportion of all possible interactions that are in fact realized (Jordano 1987). Nestedness measures how much the interactions of species with low degree values are proper subsets of the interactions of species from the same set that have higher degree values (Bascompte *et al.* 2003). We quantified nestedness using a metric based on overlap and decreasing fill ($NODF$), which varies from 0 (no nestedness) to 1

(perfect nestedness; Almeida-Neto *et al.* 2008; Bascompte & Jordano 2014). *NODF* was computed using the following equation:

$$NODF = \frac{\sum_{i<j}^{R_1} N_{ij} + \sum_{i<j}^{R_2} N_{ij}}{[R_1(R_1-1)/2] + [R_2(R_2-1)/2]} \quad \text{(S1)},$$

in which the sum on the left is over all pairs of species in the first set and the sum on the right is over all pairs of species in the second set. For each pair of species *i* and *j*, N_{ij} is defined in the following way:

$$\begin{cases} N_{ij} = \frac{n_{ij}}{\min(k_i, k_j)}, & \text{if } k_i \neq k_j \\ N_{ij} = 0, & \text{if } k_i = k_j \end{cases} \quad \text{(S2)},$$

in which n_{ij} is the number of common interactions between *i* and *j*. Finally, modularity measures how much the network is partitioned in groups of species (i.e. modules) with many interactions within groups and few interactions among different groups (Olesen *et al.* 2007). We quantified modularity using the metric *Q*, which varies from 0 (no modularity) to 1 (perfect modularity; Barber 2007; Marquitti *et al.* 2014). The metric *Q* has the following equation:

$$Q = \sum_{i=1}^{M} \left[\frac{I_i}{I} - \left(\frac{k_{1,i} k_{2,i}}{I^2} \right) \right] \quad \text{(S3)},$$

in which *M* is the number of modules in the network, I_i is the number of interactions within module *i*, *I* is the total number of interactions in the network, and $k_{1,i}$ is the sum of the degrees of species in the first set ($k_{2,i}$ for species in the second set). Each partition of a network in modules renders a different value of *Q*. Thus, we used an optimization algorithm based on simulated annealing that numerically maximizes *Q* and finds the partition that best reflects the organization of the network in modules (Marquitti *et al.* 2014).

Nestedness and modularity are known to be affected by other network properties such as species richness, degree variance, and connectance (Bascompte *et al.* 2003; Fortuna *et al.* 2010). We used a null model approach to calculate standardized values for *NODF* and *Q* and control for the effects of other metrics. We first generated 100 matrices according to the null model 2 of Bascompte *et al.* (2003) for each of our 72 empirical mutualistic networks. The matrices generated by this null

model maintain the species richness and the total number of interactions of the original empirical matrix. This null model also maintains the heterogeneity in species degrees by using the following probability of assigning 1 to the interaction between species *k* and *l*:

$$p_{kl} = \frac{1}{2}\left(\frac{\sum_i^{R_1} a_{il}}{R_1} + \frac{\sum_j^{R_2} a_{kj}}{R_2}\right) \quad \text{(S4)}.$$

Using our 100 generated matrices, we calculated standardized *NODF* values as $(NODF_{emp} - \overline{NODF}_{null})/\sigma_{NODF_{null}}$, in which $NODF_{emp}$ is the *NODF* value of the empirical matrix, $\overline{NODF}_{null}$ is the mean *NODF* value for the set of 100 matrices and $\sigma_{NODF_{null}}$ is the standard deviation of the *NODF* values of these 100 matrices. We calculated standardized *Q* values in an analogous manner.

Tables and figures

Table S1. Our dataset of 72 empirical mutualistic networks and their structural aspects. Each network is composed of two sets of species (e.g. pollinators and plants) that are placed in the rows or columns of a bipartite adjacency matrix. We calculated each structural metric using these bipartite adjacency matrices. The calculation of each metric is described below (see Network metrics). Intimacy = degree of interaction intimacy (see main text); Mutualism = mutualism type (see main text); *R* = species richness; *C* = connectance; σ_k^2 = degree variance; *NODF* = standardized nestedness; *Q* = standardized modularity; *PC1* and *PC2* = scores of first two principal components obtained via a principal components analysis. Availability: IWDB = dataset available for download at https://www.nceas.ucsb.edu/interactionweb/; Web of life = dataset available for download at http://www.web-of-life.es/; Rico-Gray = dataset kindly provided by Victor Rico-Gray; Izzo = dataset kindly provided by Thiago Izzo; Sazima = dataset kindly provided by Cristina and Ivan Sazima.

Network	Intimacy	Mutualism	Location	Rows	Columns	*R*	*C*	σ_k^2	*NODF*	*Q*	*PC1*	*PC2*	Reference	Availability
1	Low	Ant-EFN	Mexico	10	38	48	0.25	18.3	3.5	-0.19	-0.01	0.4	Guimarães *et al.* 2007a	Rico-Gray
2	Low	Ant-EFN	Mexico	28	99	127	0.1	58.37	13.58	3.11	2.93	-1.63	Guimarães *et al.* 2007a	Rico-Gray
3	Low	Ant-EFN	Mexico	5	12	17	0.22	0.89	-1.9	2.56	-1.93	-1.17	Guimarães *et al.* 2007a	Rico-Gray
4	Low	Ant-EFN	Australia	41	51	92	0.14	39.5	17.13	-2.48	3.34	1.09	Blüthgen *et al.* 2004	IWDB
5	Low	Ant-EFN	Mexico	13	46	59	0.21	20.43	4.32	3.51	-0.33	-1.53	Guimarães *et al.* 2007a	Rico-Gray
6	Low	Cleaner-client	Virgin Islands	4	32	36	0.41	20.85	1.53	0.78	-0.88	0.87	Johnson & Ruben 1988	IWDB
7	Low	Cleaner-client	Brazil	5	35	40	0.42	35.05	5.31	-1.39	0.37	2.1	Guimarães *et al.* 2007b	Sazima

Network	Intimacy	Mutualism	Location	Rows	Columns	*R*	*C*	σ_k^2	*NODF*	*Q*	*PC1*	*PC2*	Reference	Availability
8	Low	Cleaner-client	Netherlands Antilles	6	50	56	0.35	46.59	6.26	-0.87	1.05	1.61	Wicksten 1998	IWDB
9	Low	Pollinator-plant	Chile	101	87	188	0.04	23.58	14.6	0.93	3.49	-1.76	Arroyo *et al.* 1982	IWDB
10	Low	Pollinator-plant	Chile	64	42	106	0.07	12.22	8.61	0.87	1.38	-1.35	Arroyo *et al.* 1982	IWDB
11	Low	Pollinator-plant	Chile	28	41	69	0.08	8.38	5.42	1.41	0.31	-1.44	Arroyo *et al.* 1982	IWDB
12	Low	Pollinator-plant	Canada	102	12	114	0.14	47.87	9.24	-0.22	2.55	-0.06	Barrett & Helenurm 1987	Web of Life
13	Low	Pollinator-plant	Brazil	13	13	26	0.42	14.1	6.48	-0.78	-0.36	1.64	Bezerra *et al.* 2009	Web of Life
14	Low	Pollinator-plant	United Kingdom	61	17	78	0.14	40.61	11.26	-0.98	2.24	0.45	Dicks *et al.* 2002	IWDB
15	Low	Pollinator-plant	United Kingdom	36	16	52	0.15	14.16	5.45	-0.53	0.45	-0.03	Dicks *et al.* 2002	IWDB
16	Low	Pollinator-plant	Spain	38	11	49	0.26	16	2.45	0.31	-0.29	0.16	Dupont *et al.* 2003	IWDB
17	Low	Pollinator-plant	Sweden	118	23	141	0.09	22.54	7.23	0.88	1.93	-1.34	Elberling & Olesen 1999	Web of Life
18	Low	Pollinator-plant	Canada	86	29	115	0.07	28.07	10.8	-0.95	2.5	-0.31	Hocking 1968	IWDB
19	Low	Pollinator-plant	Australia	91	42	133	0.07	21.33	12.38	-0.8	2.71	-0.55	Inouye & Pyke 1988	Web of Life
20	Low	Pollinator-plant	Mauritius	100	58	158	0.09	66.81	24.08	-3.33	5.98	1.35	Kaiser-Bunbury *et al.* 2010	IWDB
21	Low	Pollinator-plant	Argentina	45	21	66	0.09	9.05	4.32	1.52	0.12	-1.44	Medan *et al.* 2002	Web of Life
22	Low	Pollinator-plant	Argentina	72	23	95	0.08	20.51	8.67	0.37	1.54	-0.92	Medan *et al.* 2002	Web of Life
23	Low	Pollinator-plant	Canada	19	11	30	0.23	7.44	3.24	-0.23	-0.52	0.29	Mosquin & Martin 1967	Web of Life
24	Low	Pollinator-plant	Mauritius	13	14	27	0.29	7.13	3.16	-0.26	-0.69	0.57	Olesen *et al.* 2002	Web of Life
25	Low	Pollinator-plant	Portugal	12	10	22	0.25	3.06	0.99	0.47	-1.16	-0.01	Olesen *et al.* 2002	Web of Life
26	Low	Pollinator-plant	South Africa	56	9	65	0.2	24.96	4.77	0.27	0.55	-0.04	Ollerton *et al.* 2003	Web of Life
27	Low	Pollinator-plant	New Zealand	60	18	78	0.11	8.2	1.51	1.87	-0.17	-1.6	Primack 1983	Web of Life
28	Low	Pollinator-plant	Venezuela	53	28	81	0.07	5.34	2.43	0.22	0.3	-1.07	Ramírez & Brito 1992	IWDB
29	Low	Pollinator-plant	Brazil	25	51	76	0.15	32.61	11.35	-2.66	2.31	1.16	Santos *et al.* 2010	IWDB
30	Low	Pollinator-plant	United States	32	7	39	0.26	20.03	5.92	-0.88	0.28	0.89	Schemske *et al.* 1978	Web of Life
31	Low	Pollinator-plant	Canada	34	13	47	0.32	20.09	1.09	-1.11	-0.23	1.17	Small 1976	Web of Life
32	Low	Pollinator-plant	Argentina	29	10	39	0.15	9.69	4.56	0.16	-0.07	-0.34	Vázquez & Simberloff 2003	Web of Life
33	Low	Pollinator-plant	Argentina	33	9	42	0.15	7.05	2.88	1.38	-0.53	-0.96	Vázquez & Simberloff 2003	Web of Life
34	Low	Pollinator-plant	Argentina	29	10	39	0.14	9.82	3.56	0.89	-0.31	-0.7	Vázquez & Simberloff 2003	Web of Life
35	Low	Pollinator-plant	Argentina	26	8	34	0.17	6.77	3.06	0.48	-0.5	-0.39	Vázquez & Simberloff 2003	Web of Life
36	Low	Pollinator-plant	Argentina	27	8	35	0.22	8.16	2.46	1.02	-0.72	-0.4	Vázquez & Simberloff 2003	Web of Life
37	Low	Frugivore-plant	United States	21	7	28	0.34	9.74	2.65	-0.3	-0.78	0.89	Baird 1980	Web of Life
38	Low	Frugivore-plant	Papua New Guinea	9	31	40	0.43	28.56	5.75	-0.79	0.11	1.79	Beehler 1983	Web of Life
39	Low	Frugivore-plant	Puerto Rico	16	25	41	0.17	10.82	7.46	-0.99	0.47	0.34	Carlo *et al.* 2003	IWDB

Network	Intimacy	Mutualism	Location	Rows	Columns	*R*	*C*	σ_k^2	*NODF*	*Q*	*PC1*	*PC2*	Reference	Availability
40	Low	Frugivore-plant	Puerto Rico	20	34	54	0.14	17.58	8.43	-1.51	1.1	0.46	Carlo *et al.* 2003	IWDB
41	Low	Frugivore-plant	Puerto Rico	13	25	38	0.15	6.36	4.23	0.71	-0.32	-0.62	Carlo *et al.* 2003	IWDB
42	Low	Frugivore-plant	Puerto Rico	15	21	36	0.16	6.6	4.68	0.03	-0.19	-0.23	Carlo *et al.* 2003	IWDB
43	Low	Frugivore-plant	Australia	7	72	79	0.28	59.52	7.55	-1.16	2.05	1.47	Crome 1975	Web of Life
44	Low	Frugivore-plant	Brazil	46	45	91	0.13	23.76	9.63	4.12	0.84	-2.27	Donatti *et al.* 2011	Web of Life
45	Low	Frugivore-plant	Brazil	29	35	64	0.14	15.93	8.29	-0.61	0.99	-0.01	Galetti and Pizo 1996	Web of Life
46	Low	Frugivore-plant	Spain	17	16	33	0.44	17.85	8.44	1.3	-0.4	0.85	Jordano 1985	Jordano
47	Low	Frugivore-plant	Mexico	27	5	32	0.64	32.63	0.98	0.51	-1.14	2.3	Kantak 1979	Web of Life
48	Low	Frugivore-plant	Malaysia	61	25	86	0.34	83.68	11.72	1.61	2.59	0.81	Lambert 1987	Web of Life
49	Low	Frugivore-plant	Papua New Guinea	32	29	61	0.07	3.47	3.22	0.52	0.02	-1.12	Mack & Wright 1996	Web of Life
50	Low	Frugivore-plant	Panama	19	4	23	0.43	9.12	0.98	0.67	-1.45	0.92	Poulin *et al.* 1999	IWDB
51	Low	Frugivore-plant	Panama	11	13	24	0.37	9.12	4.62	-1.07	-0.56	1.44	Poulin *et al.* 1999	IWDB
52	Low	Frugivore-plant	Kenya	88	33	121	0.14	58.97	12.91	-0.77	3.43	0.4	Schleuning *et al.* 2011	IWDB
53	Low	Frugivore-plant	United Kingdom	14	11	25	0.3	5.73	1.57	-0.27	-0.96	0.61	Sorensen 1981	IWDB
54	High	Anemone-fish	Indonesia	4	4	8	0.44	1.36	1.18	0.82	-1.87	0.85	Ricciardi *et al.* 2010	IWDB
55	High	Anemone-fish	Indonesia	5	4	9	0.3	0.25	0.12	1	-1.72	0.03	Ricciardi *et al.* 2010	IWDB
56	High	Anemone-fish	Indonesia	4	4	8	0.44	0.5	-0.97	0.61	-2.09	0.9	Ricciardi *et al.* 2010	IWDB
57	High	Anemone-fish	Indonesia	4	4	8	0.38	0.29	-0.85	0.74	-1.96	0.52	Ricciardi *et al.* 2010	IWDB
58	High	Anemone-fish	Indonesia	5	5	10	0.32	0.49	-0.53	0.56	-1.74	0.33	Ricciardi *et al.* 2010	IWDB
59	High	Anemone-fish	Indonesia	5	4	9	0.35	0.28	-1.4	0.6	-1.93	0.45	Ricciardi *et al.* 2010	IWDB
60	High	Anemone-fish	Indonesia	5	6	11	0.33	1.36	0.57	0.33	-1.57	0.52	Ricciardi *et al.* 2010	IWDB
61	High	Anemone-fish	Indonesia	5	4	9	0.4	0.69	-0.16	0.79	-1.93	0.64	Ricciardi *et al.* 2010	IWDB
62	High	Anemone-fish	Indonesia	4	3	7	0.5	0.24	-1.65	0.12	-2.23	1.44	Ricciardi *et al.* 2010	IWDB
63	High	Anemone-fish	Indonesia	4	4	8	0.44	0.5	-0.22	0.24	-1.94	1.08	Ricciardi *et al.* 2010	IWDB
64	High	Anemone-fish	Indonesia	3	5	8	0.47	0.5	-0.07	0.66	-2.06	1.04	Ricciardi *et al.* 2010	IWDB
65	High	Ant-myrmecophyte	Brazil	6	5	11	0.23	0.22	0.37	1.88	-1.68	-0.72	Guimarães *et al.* 2007a	Izzo
66	High	Ant-myrmecophyte	Brazil	9	7	16	0.17	0.25	0.02	2.19	-1.58	-1.19	Guimarães *et al.* 2007a	Izzo
67	High	Ant-myrmecophyte	Brazil	13	8	21	0.16	0.85	0.45	1.4	-1.28	-0.9	Guimarães *et al.* 2007a	Izzo
68	High	Ant-myrmecophyte	Brazil	8	7	15	0.16	0.31	-1.06	2.39	-1.72	-1.36	Guimarães *et al.* 2007a	Izzo
69	High	Ant-myrmecophyte	Brazil	12	9	21	0.15	0.46	-1.95	2.63	-1.75	-1.58	Guimarães *et al.* 2007a	Izzo
70	High	Ant-myrmecophyte	Peru	10	8	18	0.15	0.47	-0.48	2.26	-1.56	-1.36	Guimarães *et al.* 2007a	Izzo
71	High	Ant-myrmecophyte	Brazil	16	8	24	0.15	0.86	-1.45	2.77	-1.67	-1.65	Davidson *et al.* 1989	IWDB
72	High	Ant-myrmecophyte	Brazil	25	16	41	0.12	2.38	0.28	2.59	-1.11	-1.76	Fonseca & Ganade 1996	IWDB

Table S2. Results of the linear mixed models with the network-level trait matching as the response variable, gene flow ($\bar{g}$ = 0 and $\bar{g}$ = 0.1) and mutualism type as predictor variables, and the network identity as a random effect. For these analyses we used the following selection mosaic scenarios: two hotspots ($\overline{m}_A$ = $\overline{m}_B$ = 0.9) and one hotspot and one coldspot ($\overline{m}_A$ = 0.9, $\overline{m}_B$ = 0.1). Model: the formula for the linear mixed model as used in the R function lmer (Bates *et al.* 2015; R Core Team 2016); $\bar{\tau}_{\text{hot},n=100}$ = mean value for 100 simulations per network of the network-level trait matching at the hotspot (locality *A*); $\bar{\tau}_{\text{cold},n=100}$ = mean value for 100 simulations per network of the network-level trait matching at the coldspot (locality *B*). AIC: Akaike information criterion; Log lik: log likelihood; χ^2: chi-squared value, which is equal to two times the difference between the log likelihood of two nested models; Df: degrees of freedom for the chi-squared test, which corresponds to the difference in the number of factors of two nested models.

Model	Selection mosaic	AIC	Log lik	χ^2	Df	p
$\bar{\tau}_{\text{hot},n=100}$ ~ (1|network)	hotspot/ hotspot	-210.66	108.33			
$\bar{\tau}_{\text{hot},n=100}$ ~ $\bar{g}$ + (1|network)	hotspot/ hotspot	-320.3	164.15	111.64	1	< 0.0001
$\bar{\tau}_{\text{hot},n=100}$ ~ $\bar{g}$ + mutualism + (1|network)	hotspot/ hotspot	-370.21	194.11	59.92	5	< 0.0001
$\bar{\tau}_{\text{hot},n=100}$ ~ $\bar{g}$ + mutualism + $\bar{g}$: mutualism + (1|network)	hotspot/ hotspot	-418.46	223.23	58.24	5	< 0.0001
$\bar{\tau}_{\text{hot},n=100}$ ~ (1|network)	hotspot/ coldspot	-147.84	76.92			
$\bar{\tau}_{\text{hot},n=100}$ ~ $\bar{g}$ + (1|network)	hotspot/ coldspot	-393.71	200.85	247.86	1	< 0.0001
$\bar{\tau}_{\text{hot},n=100}$ ~ $\bar{g}$ + mutualism + (1|network)	hotspot/ coldspot	-452.68	235.34	68.98	5	< 0.0001
$\bar{\tau}_{\text{hot},n=100}$ ~ $\bar{g}$ + mutualism + $\bar{g}$: mutualism + (1|network)	hotspot/ coldspot	-459.9	243.95	17.22	5	0.0041
$\bar{\tau}_{\text{cold},n=100}$ ~ (1|network)	hotspot/ coldspot	-580.72	293.36			
$\bar{\tau}_{\text{cold},n=100}$ ~ $\bar{g}$ + (1|network)	hotspot/ coldspot	-863.74	435.87	285.02	1	< 0.0001
$\bar{\tau}_{\text{cold},n=100}$ ~ $\bar{g}$ + mutualism + (1|network)	hotspot/ coldspot	-917.17	467.58	63.43	5	< 0.0001
$\bar{\tau}_{\text{cold},n=100}$ ~ $\bar{g}$ + mutualism + $\bar{g}$: mutualism + (1|network)	hotspot/ coldspot	-959.61	493.81	52.44	5	< 0.0001

Table S3. Correlations between the first two principal components (*PC1* and *PC2*) obtained via a principal components analysis and our five metrics of network structure.

Network metric	*PC1*	*PC2*
Richness (R)	0.538	-0.232
Connectance (C)	-0.305	0.68
Degree variance ($\boldsymbol{\sigma_k^2}$)	0.48	0.257
Standardized nestedness ($NODF$)	0.562	0.066
Standardized modularity (Q)	-0.266	-0.643

Table S4. Results of the linear regressions with the network-level trait matching as the response variable and the first or second principal component of a PCA of network structural metrics (*PC1* or *PC2*) as the predictor variable. For these analyses we used the following selection mosaic scenarios: two hotspots ($\overline{m}_A$ = $\overline{m}_B$ = 0.9) and one hotspot and one coldspot ($\overline{m}_A$ = 0.9, $\overline{m}_B$ = 0.1). We performed regressions separately for three values of mean gene flow ($\bar{g}$ = 0, $\bar{g}$ = 0.01, and $\bar{g}$ = 0.1) and for each degree of interaction intimacy (high- and low-intimacy mutualisms). We only used $\bar{g}$ = 0 and $\bar{g}$ = 0.1 for the scenario with one hotspot and one coldspot because results for $\bar{g}$ = 0 and $\bar{g}$ = 0.01 were similar. $\bar{\tau}_{\text{hot},n=100}$ = mean value for 100 simulations per network of the network-level trait matching at the hotspot (locality *A*); $\bar{\tau}_{\text{cold},n=100}$ = mean value for 100 simulations per network of the network-level trait matching at the coldspot (locality *B*). Df: factor and error degrees of freedom. P-values smaller than 0.05 are in bold.

Variables	Selection mosaic	Gene flow	Intimacy	Slope	R^2	F	Df	p
$\bar{\tau}_{\text{hot},n=100} \sim PC1$	hotspot/ hotspot	0	low	-0.022	0.145	8.641	1, 51	**0.005**
$\bar{\tau}_{\text{hot},n=100} \sim PC1$	hotspot/ hotspot	0	high	0.017	0.008	0.142	1, 17	0.711
$\bar{\tau}_{\text{hot},n=100} \sim PC1$	hotspot/ hotspot	0.01	low	-0.019	0.164	9.979	1, 51	**0.003**
$\bar{\tau}_{\text{hot},n=100} \sim PC1$	hotspot/ hotspot	0.01	high	0.013	0.008	0.135	1, 17	0.718
$\bar{\tau}_{\text{hot},n=100} \sim PC1$	hotspot/ hotspot	0.1	low	-0.003	0.02	1.044	1, 51	0.312
$\bar{\tau}_{\text{hot},n=100} \sim PC1$	hotspot/ hotspot	0.1	high	0.004	0.001	0.023	1, 17	0.882
$\bar{\tau}_{\text{hot},n=100} \sim PC2$	hotspot/ hotspot	0	low	-0.034	0.17	10.46	1, 51	**0.002**
$\bar{\tau}_{\text{hot},n=100} \sim PC2$	hotspot/ hotspot	0	high	-0.022	0.233	5.168	1, 17	**0.036**
$\bar{\tau}_{\text{hot},n=100} \sim PC2$	hotspot/ hotspot	0.01	low	-0.027	0.18	11.24	1, 51	**0.001**
$\bar{\tau}_{\text{hot},n=100} \sim PC2$	hotspot/ hotspot	0.01	high	-0.019	0.248	5.598	1, 17	**0.03**
$\bar{\tau}_{\text{hot},n=100} \sim PC2$	hotspot/ hotspot	0.1	low	-0.016	0.23	15.2	1, 51	**0.0003**
$\bar{\tau}_{\text{hot},n=100} \sim PC2$	hotspot/ hotspot	0.1	high	-0.015	0.254	5.798	1, 17	**0.028**

Variables	Selection mosaic	Gene flow	Intimacy	Slope	R^2	F	Df	p
$\bar{\tau}_{\text{hot},n=100} \sim PC1$	hotspot/ coldspot	0	low	-0.024	0.162	9.871	1, 51	**0.003**
$\bar{\tau}_{\text{hot},n=100} \sim PC1$	hotspot/ coldspot	0	high	0.011	0.003	0.054	1, 17	0.818
$\bar{\tau}_{\text{hot},n=100} \sim PC1$	hotspot/ coldspot	0.1	low	-0.016	0.206	13.22	1, 51	**0.0006**
$\bar{\tau}_{\text{hot},n=100} \sim PC1$	hotspot/ coldspot	0.1	high	0.00001	0	0	1, 17	0.999
$\bar{\tau}_{\text{hot},n=100} \sim PC2$	hotspot/ coldspot	0	low	-0.033	0.162	9.877	1, 51	**0.003**
$\bar{\tau}_{\text{hot},n=100} \sim PC2$	hotspot/ coldspot	0	high	-0.022	0.226	4.955	1, 17	**0.04**
$\bar{\tau}_{\text{hot},n=100} \sim PC2$	hotspot/ coldspot	0.1	low	-0.022	0.189	11.89	1, 51	**0.001**
$\bar{\tau}_{\text{hot},n=100} \sim PC2$	hotspot/ coldspot	0.1	high	-0.015	0.138	2.717	1, 17	0.118
$\bar{\tau}_{\text{cold},n=100} \sim PC1$	hotspot/ coldspot	0	low	-0.001	0.147	8.78	1, 51	**0.005**
$\bar{\tau}_{\text{cold},n=100} \sim PC1$	hotspot/ coldspot	0	high	0.009	0.114	2.193	1, 17	0.157
$\bar{\tau}_{\text{cold},n=100} \sim PC1$	hotspot/ coldspot	0.1	low	-0.003	0.169	10.41	1, 51	**0.002**
$\bar{\tau}_{\text{cold},n=100} \sim PC1$	hotspot/ coldspot	0.1	high	0.008	0.029	0.505	1, 17	0.487
$\bar{\tau}_{\text{cold},n=100} \sim PC2$	hotspot/ coldspot	0	low	-0.001	0.115	6.611	1, 51	**0.013**
$\bar{\tau}_{\text{cold},n=100} \sim PC2$	hotspot/ coldspot	0	high	-0.002	0.069	1.258	1, 17	0.278
$\bar{\tau}_{\text{cold},n=100} \sim PC2$	hotspot/ coldspot	0.1	low	-0.004	0.184	11.5	1, 51	**0.001**
$\bar{\tau}_{\text{cold},n=100} \sim PC2$	hotspot/ coldspot	0.1	high	-0.0003	0.0007	0.012	1, 17	0.915

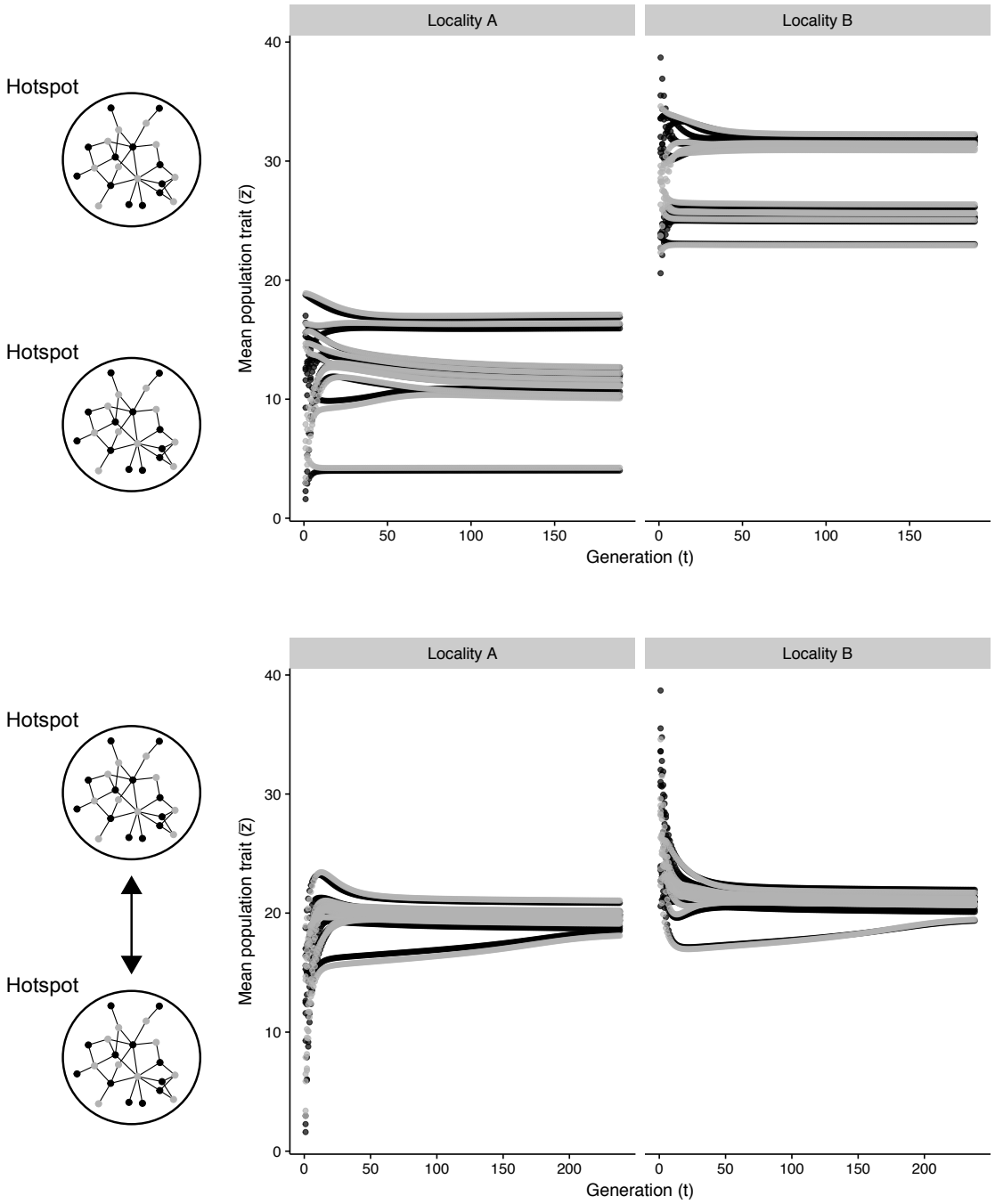

Figure S1. Examples of coevolutionary dynamics in a pollinator-plant network (network 25 in Table S1) in two isolated (top; $\bar{g}$ = 0) or connected (bottom; $\bar{g}$ = 0.1) hotspots. The trajectory of the mean trait value ($\bar{z}_i$) of all 12 pollinators (black) and 10 plants species (grey) present in the network is shown for both localities. Closer trait values indicate higher trait matching. The coevolutionary dynamics reached equilibrium when trait values stayed fixed over time. In both simulations, the mean importance of mutualistic selection was the same at both localities ($\overline{m}_A = \overline{m}_B$ = 0.9). Trait values started at the selected value in relation to the local environment ($\bar{z}_{i,A}(0) = \theta_{i,A}$ and $\bar{z}_{i,B}(0) = \theta_{i,B}$). Except for gene flow (g_i), species parameter values were the same in both simulations.

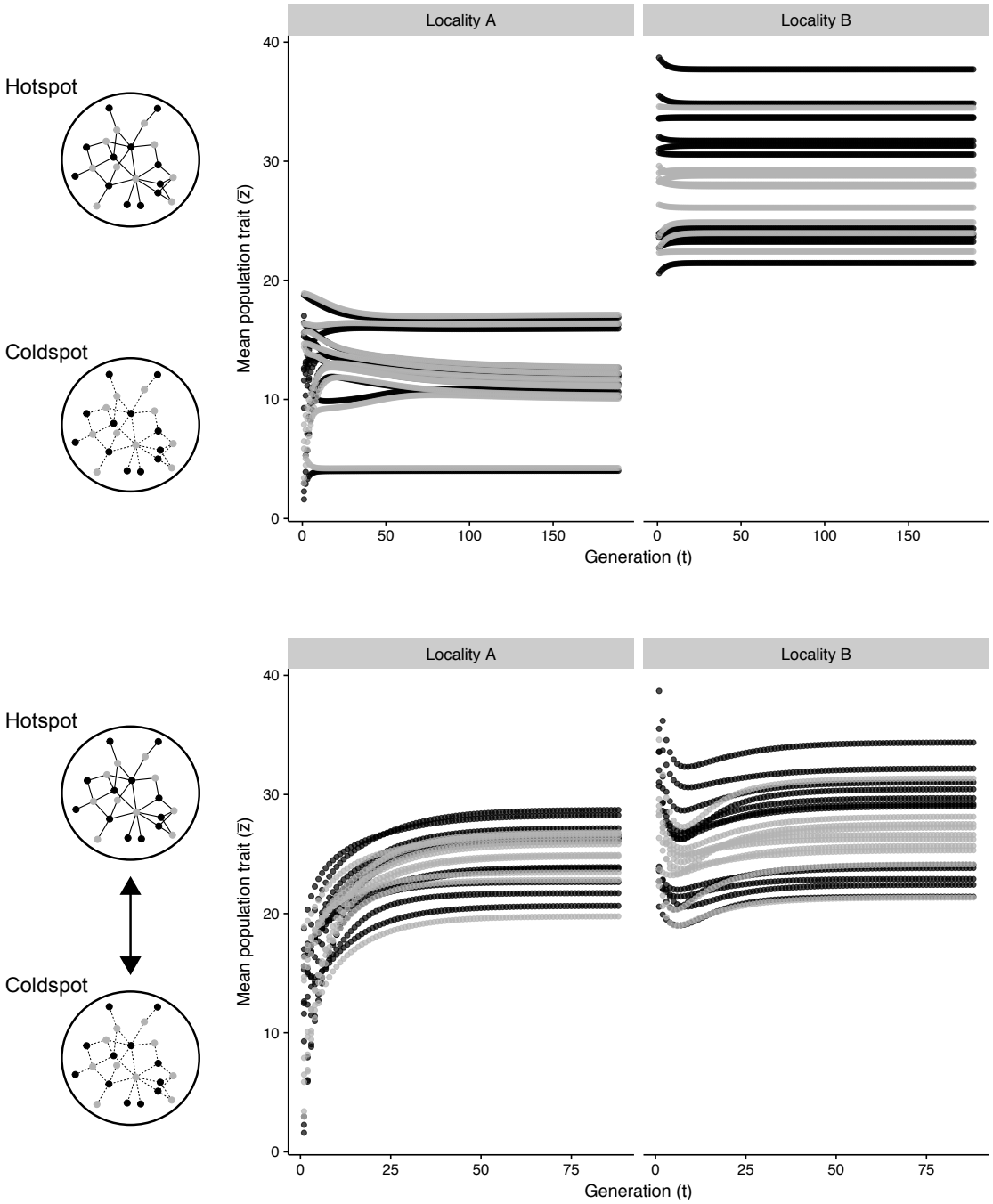

Figure S2. Examples of coevolutionary dynamics in a pollinator-plant network (network 25 in Table S1) in isolated (top; $\bar{g}$ = 0) or connected (bottom; $\bar{g}$ = 0.1) hotspot and coldspot. The trajectory of the mean trait value ($\bar{z}_i$) of all 12 pollinators (black) and 10 plants species (grey) present in the network is shown for both localities. Closer trait values indicate higher trait matching. The coevolutionary dynamics reached equilibrium when trait values stayed fixed over time. In both simulations, the mean importance of mutualistic selection was $\overline{m}_A$ = 0.9 at the hotspot and $\overline{m}_B$ = 0.1 at the coldspot. Trait values started at the selected value in relation to the local environment ($\bar{z}_{i,A}(0) = \theta_{i,A}$ and $\bar{z}_{i,B}(0) = \theta_{i,B}$). Except for gene flow (g_i), species parameter values were the same in both simulations.

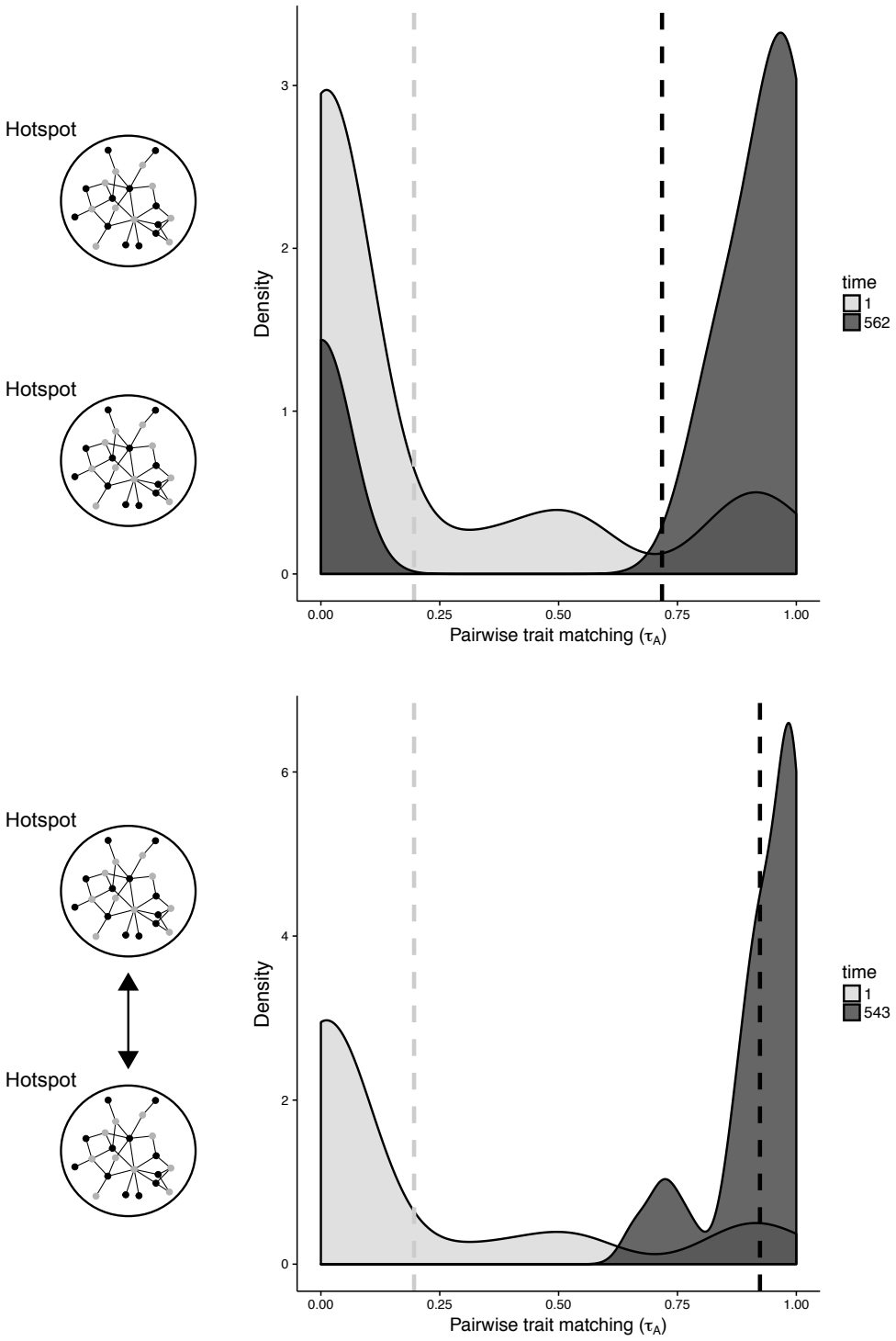

Figure S3. Changes in the distribution of pairwise trait matching (τ_{ij}) and in the network-level trait matching ($\bar{\tau}$) through coevolution in a pollinator-plant network (network 25 in Table S1) in two isolated (top; $\bar{g}$ = 0) or connected (bottom; $\bar{g}$ = 0.1) hotspots. The initial (light grey) and final (black) distribution of pairwise trait matching and value of network-level trait matching (dashed vertical line) are depicted for the two simulations. The change in the network-level trait matching occurred through a change in the distribution of pairwise trait matching. While a fraction of species pairs showed a poor final trait matching in the absence of gene flow (top; $\bar{g}$ =

0; black distribution), almost all species pairs showed an elevated final trait matching when gene flow was high (top; $\bar{g}$ = 0.1; black distribution). In both simulations, the mean importance of mutualistic selection was the same at both localities ($\overline{m}_A = \overline{m}_B$ = 0.9). Except for gene flow (g_i), species parameter values were the same in both simulations.

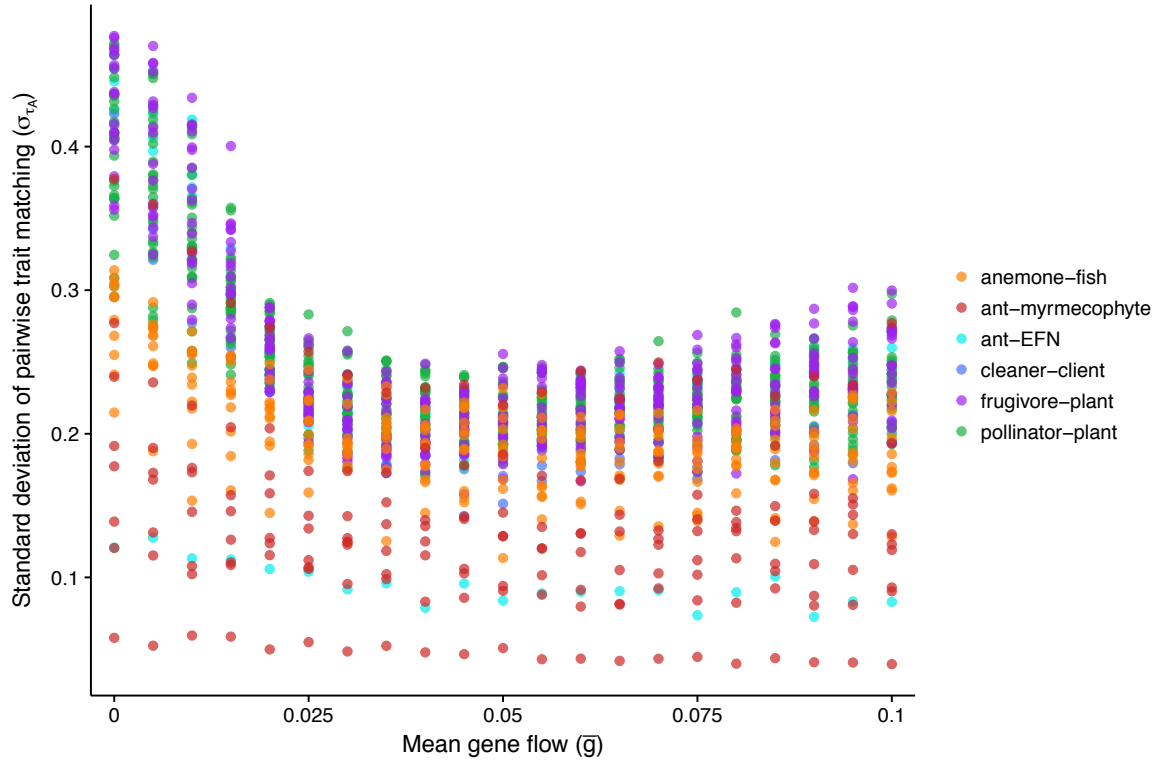

Figure S4. The effects of gene flow on the variation in pairwise trait matching (τ_{ij}) in two connected hotspots. Gene flow reduced the standard deviation of the final pairwise trait matching (σ_{τ_A}). Low-intimacy mutualisms (blue, purple, and green points) showed greater values of σ_{τ_A}. However, the decrease in σ_{τ_A} with gene flow was more pronounced in low-intimacy mutualisms as compared to high-intimacy mutualisms (orange and red points). Each point corresponds to the mean of the standard deviation of pairwise trait matching for 100 simulations for a given network ($\bar{\sigma}_{\tau_A, n=100}$). The mean importance of mutualistic selection was $\overline{m}_A = \overline{m}_B$ = 0.9.

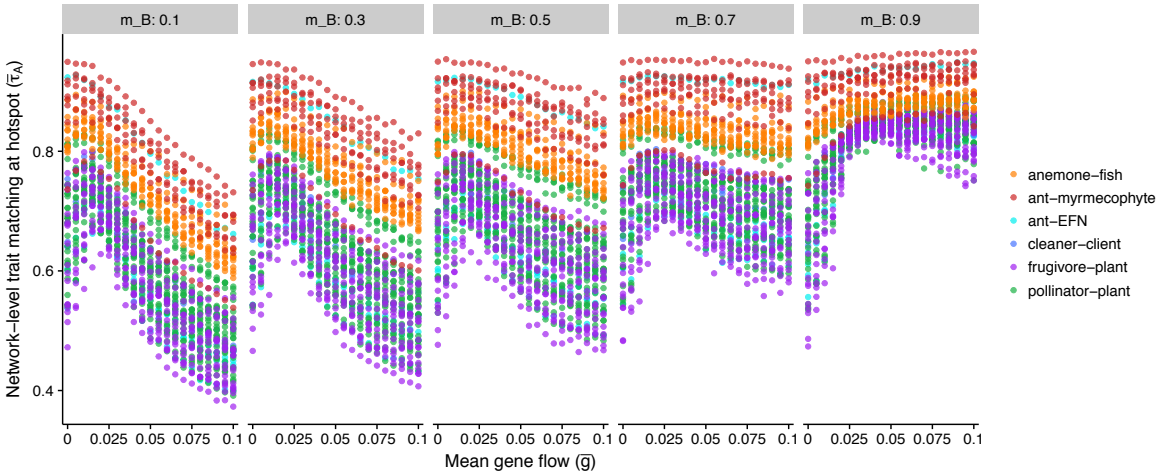

Figure S5. The effects of gene flow on the emergence of trait matching at a hotspot for different selection mosaics. Gene flow decreased the network-level trait matching ($\bar{\tau}_A$) generated by coevolution at a hotspot (locality A: $\bar{m}_A$ = 0.9) when it was connected to a coldspot (locality B: $\bar{m}_B$ = 0.1; far left; same as Fig. 2b). This effect of gene flow changes gradually as the importance of mutualistic selection increases at the coldspot ($\bar{m}_A$ = 0.9, $\bar{m}_B$ = 0.3, $\bar{m}_B$ = 0.5, $\bar{m}_B$ = 0.7, $\bar{m}_B$ = 0.9). When both localities are hotspots ($\bar{m}_A$ = 0.9, $\bar{m}_B$ = 0.9; far right; same as Fig. 2a), gene flow increased the network-level trait matching generated by coevolution. In all plots, each point corresponds to the mean of the network-level trait matching for 100 simulations for a given network ($\bar{\tau}_{A,n=100}$).

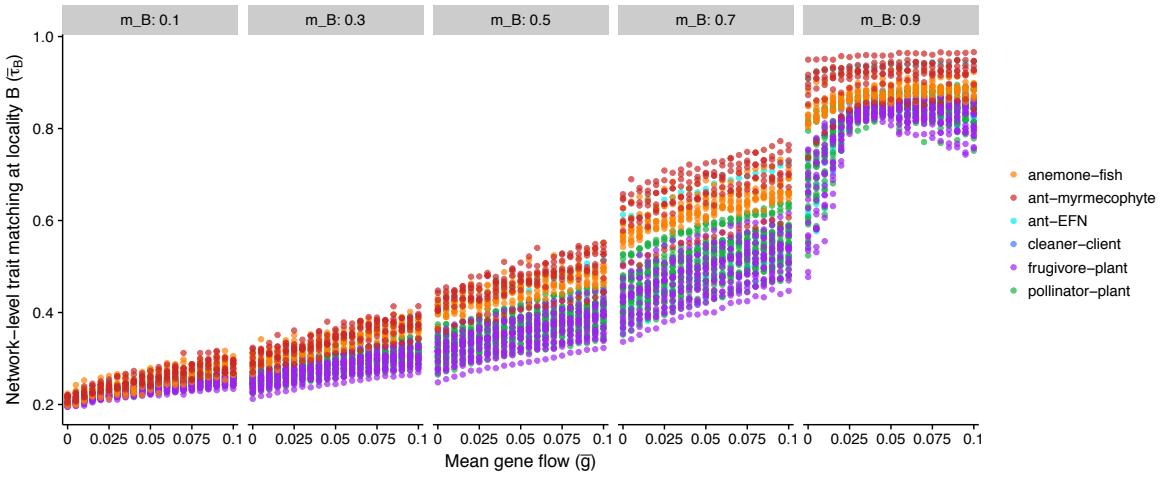

Figure S6. The effects of gene flow on the emergence of trait matching for different selection mosaics. Gene flow promoted a slight increase in the network-level trait matching ($\bar{\tau}_B$) generated by coevolution at a coldspot (locality B: $\bar{m}_B$ = 0.1) when it was connected to a hotspot (locality A: $\bar{m}_A$ = 0.9; far left; same as Fig. 2c). This effect of gene flow is gradually enhanced as the importance of mutualistic selection at locality B increases ($\bar{m}_A$ = 0.9, $\bar{m}_B$ = 0.3, $\bar{m}_B$ = 0.5, $\bar{m}_B$ = 0.7, $\bar{m}_B$ = 0.9). When both localities are hotspots ($\bar{m}_A$ = 0.9, $\bar{m}_B$ = 0.9; far right; same as Fig. 2a), gene flow increased the network-level trait matching generated by coevolution. In all plots, each point

corresponds to the mean of the network-level trait matching for 100 simulations for a given network ($\bar{\tau}_{B,n=100}$).

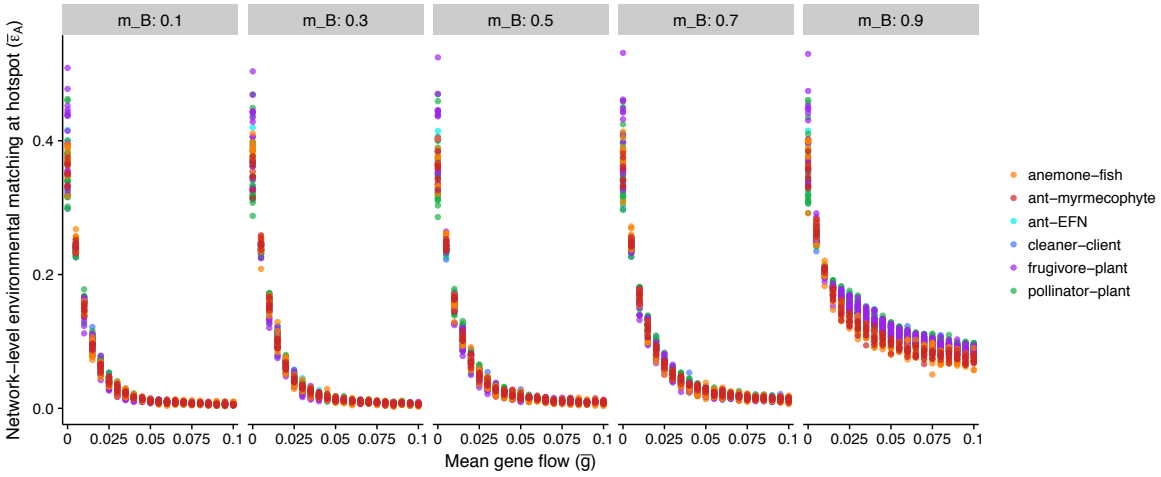

Figure S7. The effects of gene flow on environmental matching at a hotspot for different selection mosaics. Gene flow greatly decreased the network-level environmental matching ($\bar{\varepsilon}_A$) at a hotspot (locality A: $\overline{m}_A$ = 0.9) irrespective of the importance of mutualistic selection at the other locality ($\overline{m}_B$ = 0.1, $\overline{m}_B$ = 0.3, $\overline{m}_B$ = 0.5, $\overline{m}_B$ = 0.7, $\overline{m}_B$ = 0.9). When both localities were hotspots ($\overline{m}_A$ = 0.9, $\overline{m}_B$ = 0.9; far right), however, the decrease in environmental matching with gene flow was less pronounced. In all plots, each point corresponds to the mean of the network-level environmental matching for 100 simulations for a given network ($\bar{\varepsilon}_{A,n=100}$).

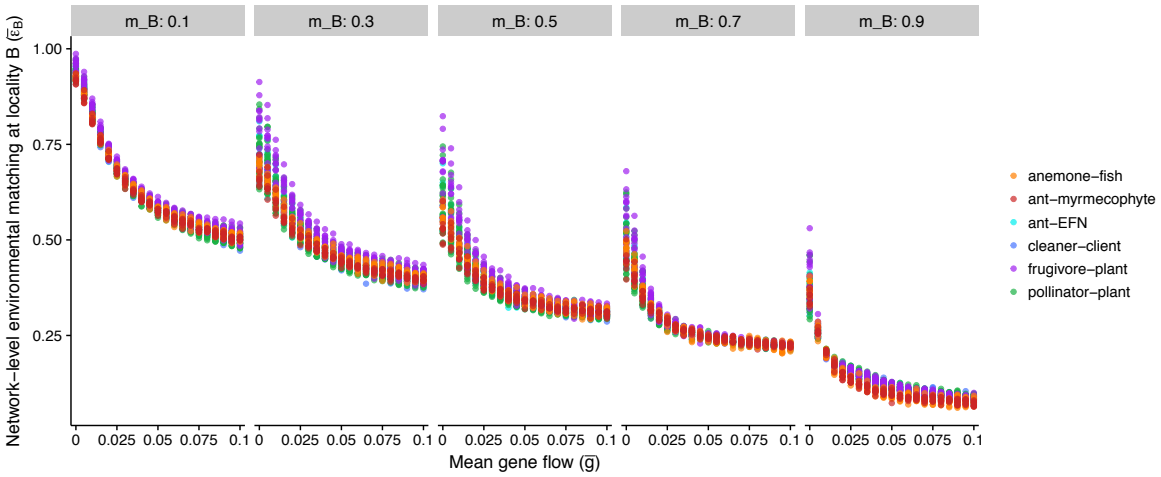

Figure S8. The effects of gene flow on environmental matching for different selection mosaics. Gene flow decreased the network-level environmental matching ($\bar{\varepsilon}_B$) at locality B irrespective of the importance of mutualistic selection at this locality ($\overline{m}_A$ = 0.9, $\overline{m}_B$ = 0.1, $\overline{m}_B$ = 0.3, $\overline{m}_B$ = 0.5, $\overline{m}_B$ = 0.7, $\overline{m}_B$ = 0.9). Although the effect of gene flow was similar for different selection mosaics, the overall level of environmental matching drops as the importance of mutualistic selection at locality B increases. In all

plots, each point corresponds to the mean of the network-level environmental matching for 100 simulations for a given network ($\bar{\varepsilon}_{B,n=100}$).

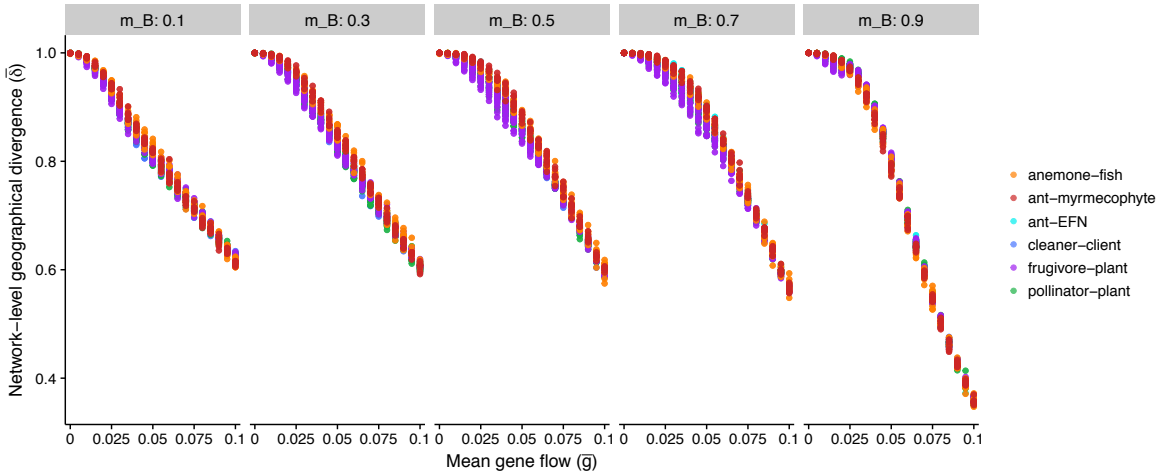

Figure S9. The effects of gene flow on the geographical divergence in species traits for different selection mosaics. Gene flow greatly decreased the network-level geographical divergence ($\bar{\delta}$) irrespective of the selection mosaic ($\overline{m}_A$ = 0.9, $\overline{m}_B$ = 0.1, $\overline{m}_B$ = 0.3, $\overline{m}_B$ = 0.5, $\overline{m}_B$ = 0.7, $\overline{m}_B$ = 0.9). This means that gene flow has an effect of homogenizing species traits across space. The decrease in geographical divergence with gene flow was stronger when both localities were hotspots ($\overline{m}_A$ = 0.9, $\overline{m}_B$ = 0.9; far right). In all plots, each point corresponds to the mean of the network-level geographical divergence for 100 simulations for a given network ($\bar{\delta}_{n=100}$).

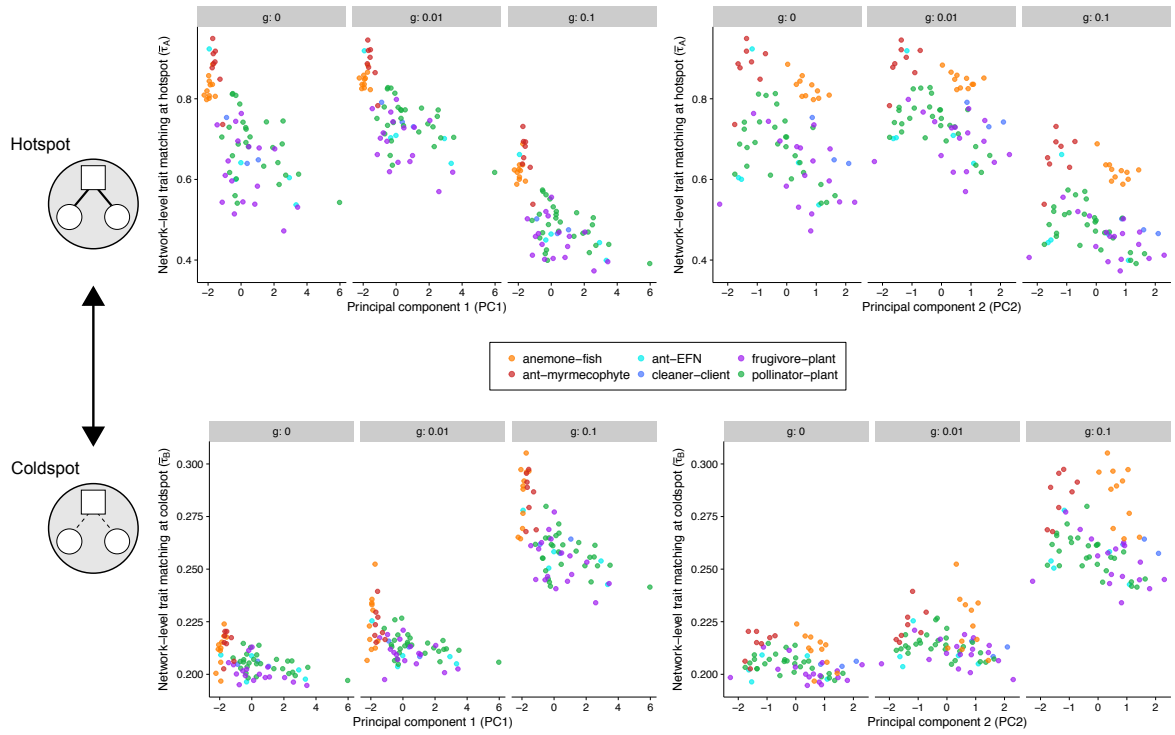

Figure S10. Mutualistic network structure mediates the effects of gene flow on coevolution when a hotspot is connected to a coldspot. Our PCA with network structure metrics showed that *PC1* was positively correlated with species richness and nestedness and *PC2* was positively correlated with connectance and negatively correlated with modularity. At the hotspot (top row), *PC1* and *PC2* affected the emergence of trait matching for $\bar{g}$ = 0 and $\bar{g}$ = 0.1 in low-intimacy mutualisms (blue, purple, and green points; Table S4). For high-intimacy mutualisms (orange and red points), only *PC2* affected the emergence of trait matching with no gene flow ($\bar{g}$ = 0; Table S4). At the coldspot (bottom row), *PC1* and *PC2* had a small effect on the emergence of trait matching for $\bar{g}$ = 0 and $\bar{g}$ = 0.1, but only for low-intimacy mutualisms (Table S4). This effect, however, was stronger with high gene flow ($\bar{g}$ = 0.1; Table S4). In all plots, each point corresponds to the mean of the network-level trait matching for 100 simulations for a given network ($\bar{\tau}_{A,n=100}$ or $\bar{\tau}_{B,n=100}$). The mean importance of mutualistic selection was $\bar{m}_A$ = 0.9 at the hotspot and $\bar{m}_B$ = 0.1 at the coldspot.

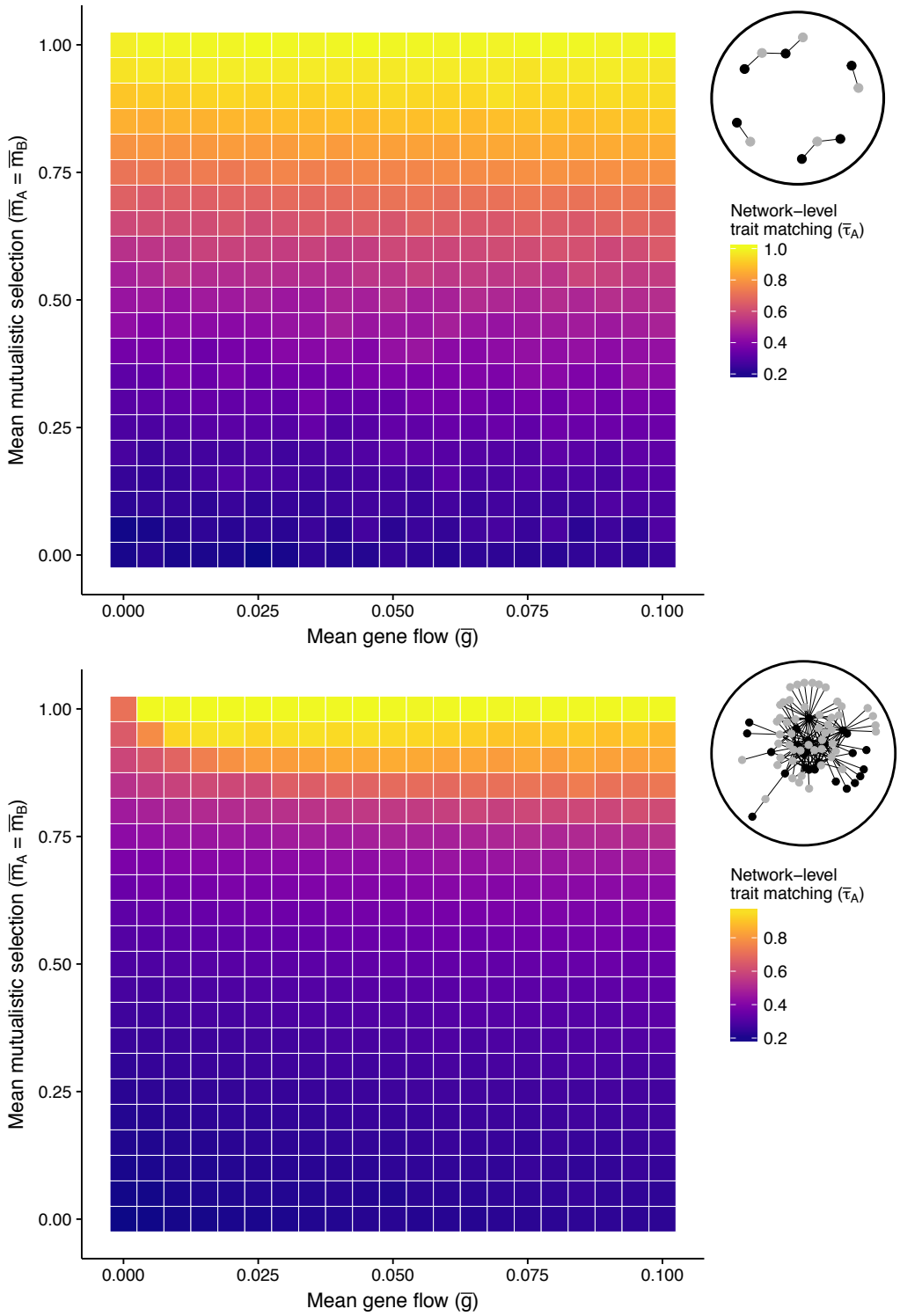

Figure S11. The combined effects of gene flow and symmetric selection mosaics on the emergence of trait matching for two networks with contrasting structures. Overall, the network-level trait matching ($\bar{\tau}_A$) was higher for the ant-myrmecophyte network (top; network 65 in Table S1) than for the pollinator-plant network (bottom; network 29 in Table S1). For the ant-myrmecophyte network (top) the network-level trait matching was mainly affected by the importance of mutualistic selection ($\overline{m}_A$ and $\overline{m}_B$) and gene flow ($\bar{g}$) had a weak effect. In contrast, for the pollinator-plant network (bottom) the network-level trait matching was affected by both the importance of

mutualistic selection and gene flow. However, the effect of gene flow was only important for high values of $\overline{m}_A$ and $\overline{m}_B$ (i.e. two connected hotspots). In these simulations, the importance of mutualistic selection was the same at both localities (symmetric selection mosaic: $\overline{m}_A = \overline{m}_B$). In both plots, the color of each square corresponds to the mean of the network-level trait matching at locality A for 100 simulations ($\bar{\tau}_{A,n=100}$). Networks depict the interactions between animal (black) and plant species (grey).

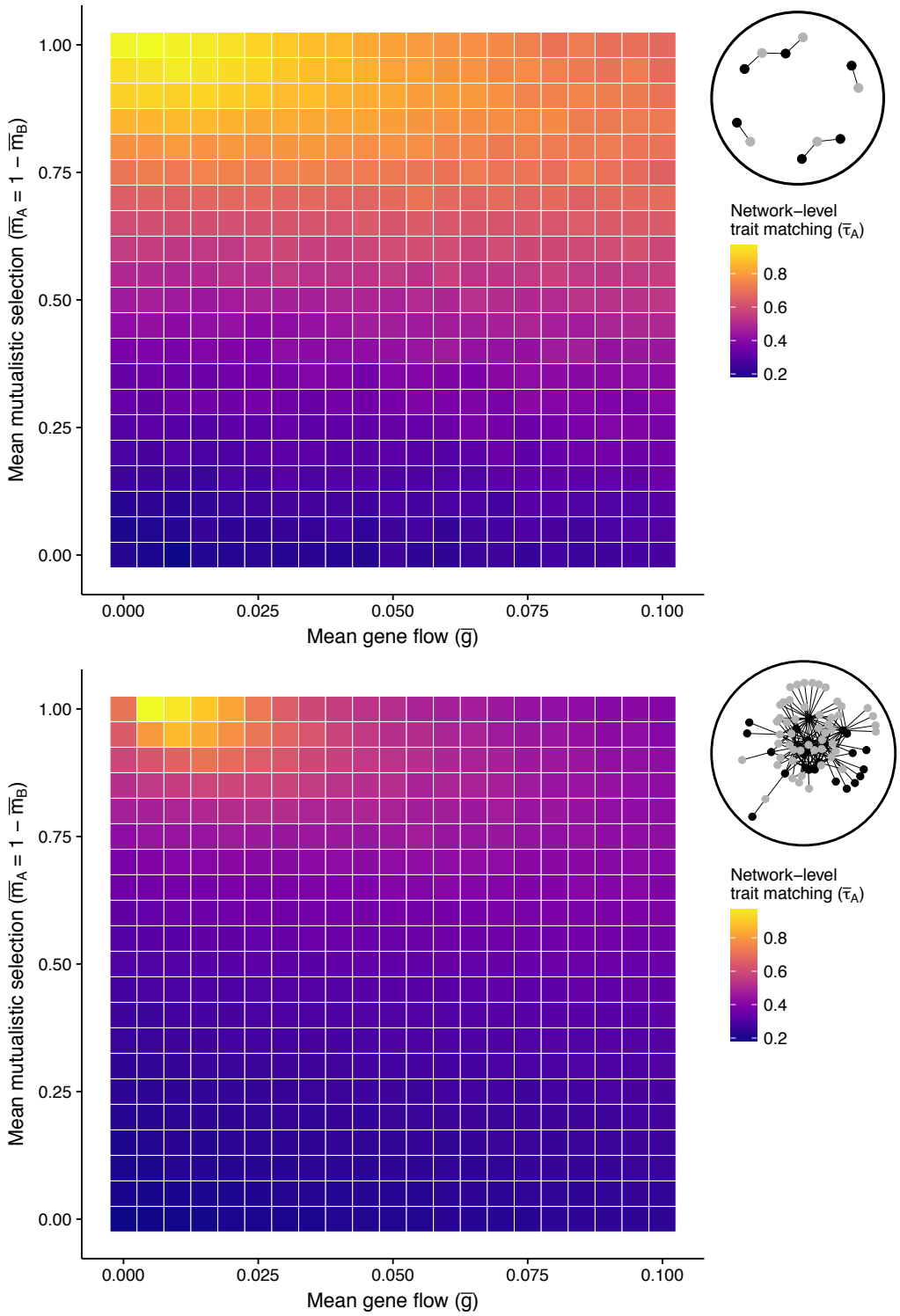

Figure S12. The combined effects of gene flow and asymmetric selection mosaics on the emergence of trait matching for two networks with contrasting structures. Overall, the network-level trait matching ($\bar{\tau}_A$) was higher for the ant-myrmecophyte network (top; network 65 in Table S1) than for the pollinator-plant network (bottom; network 29 in Table S1). However, the combination of gene flow ($\bar{g}$) and importance of mutualistic selection ($\overline{m}_A$ and $\overline{m}_B$) had a similar effect in both networks. Specifically, gene flow reduced the network-level trait matching, but only when $\overline{m}_A$ was high and $\overline{m}_B$ was low (i.e. a hotspot connected to a coldspot; top part of both plots). In these

simulations, the importance of mutualistic selection was asymmetric between localities ($\overline{m}_A$ = 1 - $\overline{m}_B$). In both plots, the color of each square corresponds to the mean of the network-level trait matching at locality A for 100 simulations ($\bar{\tau}_{A,n=100}$). Networks depict the interactions between animal (black) and plant species (grey).

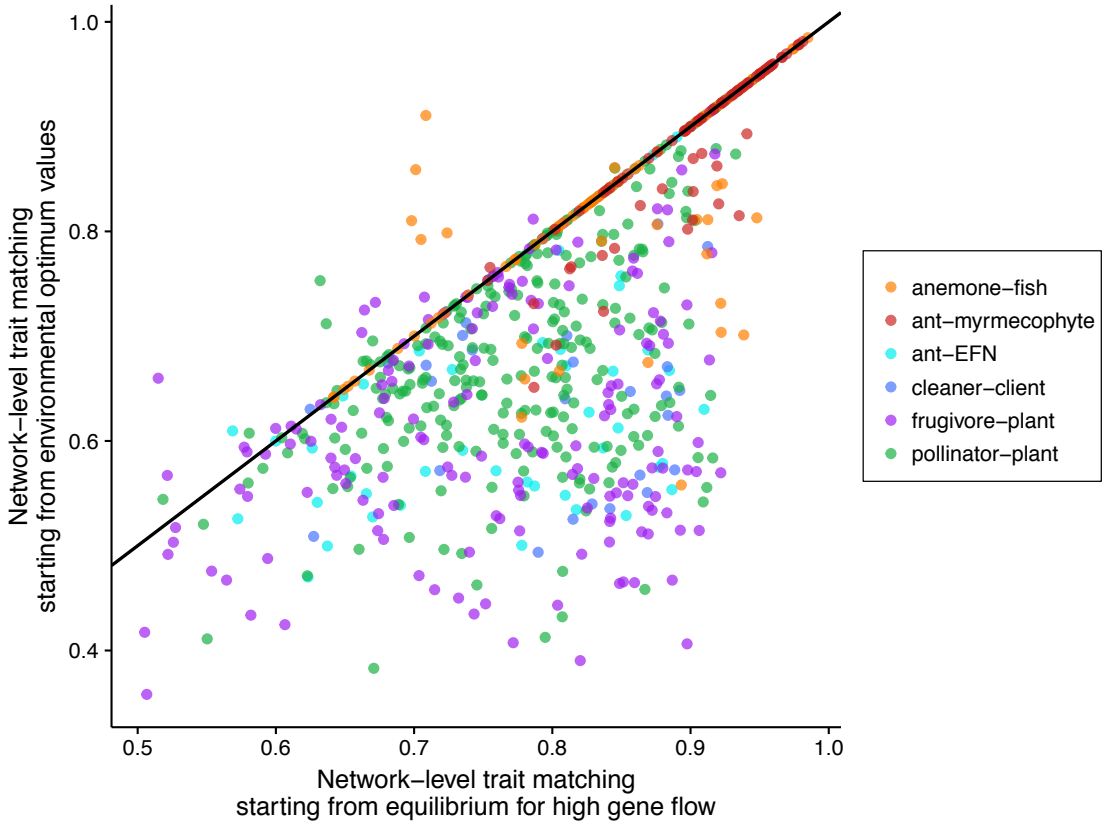

Figure S13. Influence of the initial trait values on the final value of trait matching in one isolated hotspot (i.e. $\bar{g}$ = 0). Each point represents the network-level trait matching ($\bar{\tau}_A$) of a pair of simulations with the same parameter values, but with different initial conditions (10 pairs of simulations per network: total = 1440 simulations). The y axis represents the network-level trait matching of simulations in which traits started at the environmental optimum values (i.e. $\bar{z}_{i,A}(0) = \theta_{i,A}$ and $\bar{z}_{i,B}(0) = \theta_{i,B}$). The x axis represents the network-level trait matching of simulations in which traits started at the equilibrium for the coevolutionary dynamics with high gene flow ($\bar{g}$ = 0.1). Points that fall on the black line (y = x) have the same final value of the network-level trait matching for both simulations. Points that do not fall on the black line indicate that different initial conditions generated different values of the network-level trait matching. The mean importance of mutualistic selection in these simulations was $\overline{m}_A$ = $\overline{m}_B$ = 0.9.

References

1. Almeida-Neto, M., Guimarães, P., Guimarães, P.R., Loyola, R.D. & Ulrich, W. (2008). A consistent metric for nestedness analysis in ecological systems: reconciling concept and measurement. *Oikos*, 117, 1227–1239

2. Arroyo, M.T.K., Primack, R. & Armesto, J. (1982). Community Studies in Pollination Ecology in the High Temperate Andes of Central Chile. I. Pollination Mechanisms and Altitudinal Variation. *Am. J. Bot.*, 69, 82–97

3. Baird, J.W. (1980). The Selection and Use of Fruit by Birds in an Eastern Forest. *Wilson Bull.*, 92, 63–73

4. Barber, M.J. (2007). Modularity and community detection in bipartite networks. *Phys. Rev. E*, 76, 66102

5. Barrett, S.C.H. & Helenurm, K. (1987). The reproductive biology of boreal forest herbs. I. Breeding systems and pollination. *Can. J. Bot.*, 65, 2036–2046

6. Bascompte, J. & Jordano, P. (2014). *Mutualistic Networks*. Princeton University Press, Princeton, New Jersey

7. Bascompte, J., Jordano, P., Melián, C.J. & Olesen, J.M. (2003). The nested assembly of plant–animal mutualistic networks. *Proc. Natl. Acad. Sci.*, 100, 9383–9387

8. Beehler, B. (1983). Frugivory and Polygamy in Birds of Paradise. *Am. Ornithol. Soc.*, 100, 1–12

9. Bezerra, E.L.S., MacHado, I.C. & Mello, M.A.R. (2009). Pollination networks of oil-flowers: A tiny world within the smallest of all worlds. *J. Anim. Ecol.*, 78, 1096–1101

10. Blüthgen, N., Stork, N.E. & Fiedler, K. (2004). Bottom-up control and co-occurrence in complex communities: Honeydew and nectar determine a rainforest ant mosaic. *Oikos*, 106, 344–358

11. Carlo, T., Collazo, J. & Groom, M. (2003). Avian fruit preferences across a Puerto Rican forested landscape: pattern consistency and implications for seed removal. *Oecologia*, 134, 119–131

12. Crome, F.H.J. (1975). The ecology of fruit pigeons in tropical Northern Queensland. *Wildl. Res.*, 2, 155–185

13. Davidson, D.W., Snelling, R.R. & Longino, J.T. (1989). Competition Among Ants for Myrmecophytes and the Significance of Plant Trichomes. *Biotropica*, 21, 64–73

14. Dicks, L. V, Corbet, S. a & Pywell, R.F. (2002). Compartmentalization in plant–insect flower visitor webs. *J. Anim. Ecol.*, 71, 32–43

15. Donatti, C.I., Guimarães, P.R., Galetti, M., Pizo, M.A., Marquitti, F.M.D. & Dirzo, R. (2011). Analysis of a hyper-diverse seed dispersal network: modularity and underlying mechanisms. *Ecol. Lett.*, 14, 773–781

16. Dupont, Y.L., Hansen, D.M. & Olesen, J.M. (2003). Structure of a plant–flower-visitor network in the high-altitude sub-alpine desert of Tenerife, Canary Islands. *Ecography*, 26, 301–310

17. Elberling, H. & Olesen, J. (1999). The structure of a high latitude plant-flower visitor system: the dominance of flies. *Ecography*, 22, 314–323

18. Fonseca, C.R. & Ganade, G. (1996). Asymmetries, compartments and null interactions in an Amazonian ant-plant community. *J. Anim. Ecol.*, 65, 339–347

19. Fortuna, M.A., Stouffer, D.B., Olesen, J.M., Jordano, P., Mouillot, D., Krasnov, B.R., *et al.* (2010). Nestedness versus modularity in ecological networks: two sides of the same coin? *J. Anim. Ecol.*, 79, 811–817

20. Galetti, M. & Pizo, M.A. (1996). Fruit eating birds in a forest fragment in southeastern Brazil. *Ararajuba, Rev. Bras. Ornitol.*, 4, 71–79

21. Guimarães, P.R., Rico-Gray, V., Oliveira, P.S., Izzo, T.J., dos Reis, S.F. & Thompson, J.N. (2007a). Interaction Intimacy Affects Structure and Coevolutionary Dynamics in Mutualistic Networks. *Curr. Biol.*, 17, 1797–1803

22. Guimarães, P.R., Sazima, C., dos Reis, S.F. & Sazima, I. (2007b). The nested structure of marine cleaning symbiosis: is it like flowers and bees? *Biol. Lett.*, 3, 51–54

23. Hocking, B. (1968). Insect-Flower Associations in the High Arctic with Special Reference to Nectar. *Oikos*, 19, 359–387

24. Inouye, D.W. & Pyke, G.H. (1988). Pollination biology in the Snowy Mountains of Australia: Comparisons with montane Colorado, USA. *Austral Ecol.*, 13, 191–210

25. Johnson, W.S. & Ruben, P. (1988). Cleaning behavior of Bodianus rufus, Thalassoma bifasciatum, Gobiosoma evelynae, and Periclimenes pedersoni along a depth gradient at Salt River Submarine Canyon, St. Croix. *Environ. Biol. Fishes*, 23, 225–232

26. Jordano, P. (1985). El ciclo anual de los paseriformes frugívoros en el matorral mediterráneo del sur de España: importancia de su invernada y variaciones interanuales. *Ardeola*, 32, 69–94

27. Jordano, P. (1987). Patterns of mutualistic interactions in pollination and seed dispersal: connectance, dependence asymmetries, and coevolution. *Am. Nat.*, 129, 657–677

28. Kaiser-Bunbury, C.N., Muff, S., Memmott, J., Müller, C.B. & Caflisch, A. (2010). The robustness of pollination networks to the loss of species and interactions: a

quantitative approach incorporating pollinator behaviour. *Ecol. Lett.*, 13, 442–452

29. Kantak, G.E. (1979). Observations on Some Fruit-Eating Birds in Mexico. *Auk*, 96, 183–186

30. Lambert, F. (1989). Fig-Eating by Birds in a Malaysian Lowland Rain Forest. *J. Trop. Ecol.*, 5, 401–412

31. Mack, A.L. & Wright, D.D. (1996). Notes on the nests and eggs of some birds at the Crater Mountain Research Station, Papua New Guinea. *Emu*, 96, 89–101

32. Marquitti, F.M.D., Guimarães, P.R., Pires, M.M. & Bittencourt, L.F. (2014). MODULAR: Software for the Autonomous Computation of Modularity in Large Network Sets. *Ecography*, 37, 221–224

33. Medan, D., Montaldo, N.H., Devoto, M., Mantese, A., Vasellati, V., Roitman, G.G., *et al.* (2002). Plant-Pollinator Relationships at Two Altitudes in the Andes of Mendoza, Argentina. *Arctic, Antarct. Alp. Res.*, 34, 233–241

34. Mosquin, T. & Martin, J.E.H. (1967). Observations on the pollination biology of plants on Melville Island, N.W.T., Canada. *Can. F. Nat.*, 81, 201–205

35. Olesen, J.M., Bascompte, J., Dupont, Y.L. & Jordano, P. (2007). The modularity of pollination networks. *Proc. Natl. Acad. Sci.*, 104, 19891–19896

36. Olesen, J.M., Eskildsen, L.I. & Venkatasamy, S. (2002). Invasion of pollination networks on oceanic islands: Importance of invader complexes and endemic super generalists. *Divers. Distrib.*, 8, 181–192

37. Ollerton, J., Johnson, S.D., Cranmer, L. & Kellie, S. (2003). The pollination ecology of an assemblage of grassland asclepiads in South Africa. *Ann. Bot.*, 92, 807–834

38. Poulin, B., Wright, S.J., Lefebvre, G. & Calderón, O. (1999). Interspecific synchrony and asynchrony in the fruiting phenologies of congeneric bird-dispersed plants in Panama. *J. Trop. Ecol.*, 15, 213–227

39. Primack, R.B. (1983). Insect pollination in the New Zealand mountain flora. *New Zeal. J. Bot.*, 21, 317–333

40. Ramirez, N. & Brito, Y. (1992). Pollination biology in a palm swamp community in the Venezuelan Central Plains. *Bot. J. Linn. Soc.*, 110, 277–302

41. Ricciardi, F., Boyer, M. & Ollerton, J. (2010). Assemblage and interaction structure of the anemonefish-anemone mutualism across the Manado region of Sulawesi, Indonesia. *Environ. Biol. Fishes*, 87, 333–347

42. Santos, G.M. de M., Aguiar, C.M.L. & Mello, M.A.R. (2010). Flower-visiting guild associated with the Caatinga flora: trophic interaction networks formed by social bees and social wasps with plants. *Apidologie*, 41, 466–475

43. Schemske, D.W., Willson, M.F., Melampy, M.N., Miller, L.J., Schemske, K.M. & Best, L.B. (1978). Flowering Ecology of Some Spring Woodland Herbs. *Ecology*, 59, 351–366

44. Schleuning, M., Blüthgen, N., Flörchinger, M., Braun, J., Schaefer, H.M. & Böhning-Gaese, K. (2011). Specialization and interaction strength in a tropical plant-frugivore network differ among forest strata. *Ecology*, 92, 26–36

45. Small, E. (1976). Insect pollinators of the Mer Bleue peat bog of Ottawa. *Can. field-naturalist*, 90, 22–28

46. Sorensen, A.E. (1981). Interactions between birds and fruit in a temperate woodland. *Oecologia*, 50, 242–249

47. Vázquez, D.P. & Simberloff, D. (2003). Changes in interaction biodiversity induced by an introduced ungulate. *Ecol. Lett.*, 6, 1077–1083

48. Wicksten, M.K. (1998). Behaviour of cleaners and their client fishes at Bonaire, Netherlands Antilles. *J. Nat. Hist.*, 32, 13–30